

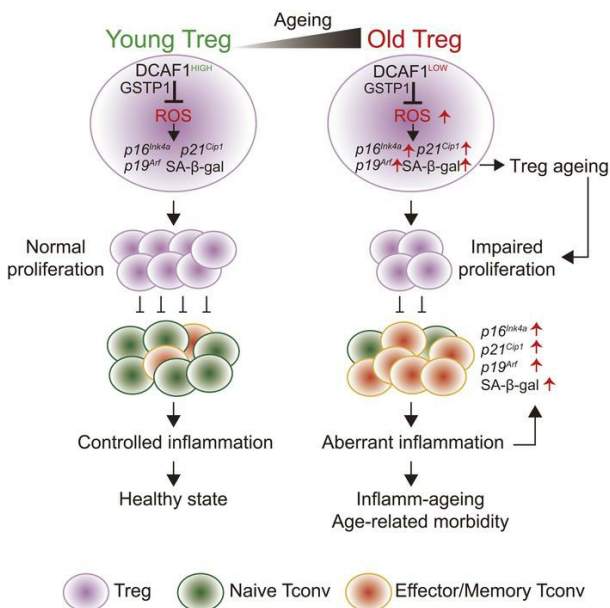
# DCAF1 regulates Treg senescence via the ROS axis during immunological ageing

Zengli Guo, ... , Jenny Pan-Yun Ting, Yisong Y. Wan

*J Clin Invest.* 2020. <https://doi.org/10.1172/JCI136466>.

Research In-Press Preview Aging Immunology

## Graphical abstract



Find the latest version:

<https://jci.me/136466/pdf>



1                   **DCAF1 regulates Treg senescence via the ROS axis during**  
2   **immunological ageing**

3 **Authors:**

4 Zengli Guo<sup>1,2</sup>, Gang Wang<sup>1,2,3</sup>, Bing Wu<sup>1,2</sup>, Wei-Chun Chou<sup>1,4</sup>, Liang Cheng<sup>1,2</sup>, Chenlin  
5 Zhou<sup>1</sup>, Jitong Lou<sup>5</sup>, Di Wu<sup>5,6</sup>, Lishan Su<sup>1,2</sup>, Junnian Zheng<sup>3</sup>, Jenny P-Y Ting<sup>1,2,4</sup>, and  
6 Yisong Y. Wan<sup>1,2\*</sup>

7 **Affiliations:**

8 <sup>1</sup>Lineberger Comprehensive Cancer Center, University of North Carolina at Chapel Hill,  
9 NC, 27599, USA; <sup>2</sup>Department of Microbiology and Immunology, University of North  
10 Carolina at Chapel Hill, NC 27599, USA; <sup>3</sup>Jiangsu Center for the Collaboration and  
11 Innovation of Cancer Biotherapy, Cancer Institute, Xuzhou Medical University, Xuzhou,  
12 Jiangsu 221002, China; <sup>4</sup>Department of Genetics, University of North Carolina at Chapel  
13 Hill, NC, 27599, USA; <sup>5</sup>Department of Biostatistics, Gillings School of Global Public  
14 Health, University of North Carolina at Chapel Hill, Chapel Hill, NC 27599, USA;  
15 <sup>6</sup>Department of Periodontology, School of Dentistry, University of North Carolina at  
16 Chapel Hill, Chapel Hill, NC 27599, USA

17 **\*Correspondence to:** Yisong Y. Wan, Lineberger Comprehensive Cancer Center,  
18 Department of Microbiology and Immunology, University of North Carolina at Chapel  
19 Hill, 125 Mason Farm Road, Chapel Hill, NC 27599-7599; Phone: 919-966-9728; Email:  
20 [wany@email.unc.edu](mailto:wany@email.unc.edu)

21 **One Sentence Summary:**

22                   Treg cell ageing driven by ROS permits aberrant T cell activation during  
23 immunological ageing.

24 **Abstract**

25           As a hallmark of immunological ageing, the low-grade, chronic inflammation  
26 with accumulation of effector-memory T cells contributes to the increased susceptibility  
27 of many ageing-related diseases. While the proinflammatory state of aged T cells  
28 indicates a dysregulation of immune homeostasis, whether and how ageing drives  
29 regulatory T (Treg) cell ageing and alters their function is not fully understood due to a  
30 lack of specific ageing markers. Here, by a combination of cellular, molecular and  
31 bioinformatic approaches, we discover that Treg cells senesce more severely than  
32 conventional T (Tconv) cells during ageing. We found Treg cells from aged mice were  
33 less efficient than young Treg cells to suppress Tconv cell function in an inflammatory-  
34 bowel-disease model and to prevent Tconv cell ageing in the irradiation-induced ageing  
35 model. Furthermore, we revealed that DCAF1 (DDB1 and CUL4 associated factor 1) was  
36 downregulated in aged Treg cells and was critical to restrain Treg cell ageing via  
37 glutathione S-transferase P (GSTP1) regulated reactive-oxygen-species (ROS).  
38 Importantly, interfering with GSTP1 and ROS pathways reinvigorated the proliferation  
39 and function of aged Treg cells. Therefore, our studies uncover an important role of  
40 DCAF1-GSTP1-ROS axis in Treg cell senescence, which leads to uncontrolled  
41 inflammation and immunological ageing.

42

43

44

45 **Introduction**

46 Immunological ageing is associated with declined immunity (immunosenescence)  
47 and chronic nonspecific inflammation (inflamm-ageing) (1), contributing to age-  
48 associated morbidities and mortalities, including infection, cancer and autoimmunity,  
49 which are detrimental to the health of ageing populations globally (2-4). Chronic  
50 inflammation not only accelerates immunological ageing (5), but also contributes to a  
51 variety of ageing-related diseases (6) such as Alzheimer's disease (7, 8). Thus, targeting  
52 chronic inflammation, by using genetic and pharmacological approaches, has been an  
53 important strategy to extend the healthspan and lifespan across species (9). As one of the  
54 most basic changes in immunological ageing, the accumulation of excessive effector-  
55 memory T cells exists in both aged humans and aged pathogen-free mice (10, 11) with  
56 poorly defined mechanisms.

57 The proper function of immune system can only be achieved by well-balanced  
58 immune activation and immune suppression, as the disruption of immune homeostasis  
59 often leads to health issues and diseases (12). Because conventional T cells (Tconv)  
60 activate immune responses and regulatory T (Treg) cells suppress them (13), effector-  
61 memory T cell accumulation during ageing could be due to either enhanced Tconv cell  
62 function or reduced Treg cell function. The former possibility seems less likely because it  
63 is generally agreed that the function of Tconv cells does not enhance, if not worsens, with  
64 ageing (14), which contributes to compromised vaccination and declined immunity  
65 against tumors and infections in aged population (15). However, the latter possibility that  
66 defects in Treg cell function lead to ageing-related inflammation remains unclearly  
67 defined (16).

68 Previous studies found that the function of aged Treg cells appeared unaltered or  
69 even increased (17-19). Yet, later studies suggested that aged Treg cells may be less  
70 effective in suppressing the function of Tconv cells *in vitro* (20) and in expanding in  
71 response to muscle injury *in vivo* (21), implying ageing may negatively influence the  
72 intrinsic function of Treg cells. Therefore, whether and how the intrinsic function of Treg  
73 cells may alter during ageing to impact immunological ageing remains a question to be  
74 clearly elucidated (22).

75 Here we investigated the intrinsic function of Treg cells during ageing and  
76 discovered that, Treg cells senesce more severely than conventional T (Tconv) cells when  
77 age, with a preferential upregulation of senescence-related molecular program.  
78 Compared to non-aged Treg cells, aged Treg cells were less efficient in proliferating and  
79 in suppressing Tconv cell function both *in vitro* and in an inflammatory-bowel-disease  
80 model. Consequently, aged Treg cells failed to prevent Tconv cell ageing in an  
81 irradiation-induced immunological ageing model when compared to young Treg cells. In  
82 addition, we discovered DCAF1 was critical to restrain Treg cell ageing by interacting  
83 with GSTP1, an important enzyme to buffer reactive-oxygen-species (ROS) by  
84 catalyzing intracellular detoxification reactions. Moreover, we revealed that ROS related  
85 program was preferentially upregulated in aged Treg cells, and importantly, interfering  
86 with GSTP1 and ROS pathways reinvigorated the proliferation and function of aged Treg  
87 cells.

88

## 89 **Results**

### 90 **Preferential Treg cell ageing compared to Tconv cells in young and aged mice.**

91 We comprehensively analyzed T cell function in aged (> 18 months old) mice.  
92 Tconv cells in aged mice adopted effector-memory phenotypes (**Fig. S1, A-D**), a  
93 hallmark of immunological ageing, as expected (10). While aged Tconv cells were not  
94 intrinsically more sensitive to TCR activated proliferation compared to their young  
95 counterparts, aged Treg cells proliferated much less than young Treg cells (**Fig. 1A**),  
96 when they were co-cultured under the same conditions to exclude cell extrinsic  
97 influences. The proliferative defect of aged Treg cells consistently existed in assays either  
98 by CFSE dilution or BrdU incorporation (**Fig. 1A and Fig. S1E**), regardless of the  
99 presence or absence of Tconv cells (**Fig. S1, F and G**) or the strength of TCR stimulation  
100 (**Fig. S1H**). This finding is quite unexpected as the proportion of Treg cells was found  
101 increased in aged mice (18, 20, 23) (**Fig. S1I**), which could be due to chronic  
102 inflammation driven Treg cell expansion (24). Consistent with the reduced proliferative  
103 capacity, aged Treg cells displayed high  $\beta$ -galactosidase (SA- $\beta$ -gal) activity (**Fig. 1B**), a  
104 hallmark for cellular senescence (25). Unbiased genome-wide RNA-seq analysis  
105 identified genes that were differentially regulated in aged Treg cells compared to their  
106 young counterparts to reveal an enrichment of ageing-related program (26) (**Fig. 1C**) and  
107 preferential upregulation of senescence signature genes including *p16<sup>Ink4a</sup>*, *p19<sup>Arf</sup>* and  
108 *p21<sup>Cip1</sup>* (**Fig. 1, D, E and Supplemental Table 1**) in aged Treg cells. Interestingly,  
109 genome-wide RNA-seq analysis also revealed that the ageing-related program was  
110 preferentially up-regulated in Treg cells when compared with Tconv cells regardless of  
111 age (**Fig. 1, E and F**), in agreement with the previous study on human T cells showing

112 that Treg cells have shorter telomere than Tconv cells in both young and old donors (19).  
113 Therefore, compared to Tconv cells, Treg cells manifest a more severe ageing phenotype  
114 with deteriorated proliferative capacity during ageing.

115

#### 116 **Deterioration of Treg cell function in aged mice.**

117 Whether and how ageing impacts Treg cell function remains unclearly defined  
118 (18, 20, 27-29). Our findings that aged Treg cells showed defective proliferation and  
119 exacerbated senescence prompted us to comprehensively evaluate the intrinsic function  
120 of aged Treg cells *in vitro* and *in vivo*. The suppression assay performed *in vitro* showed  
121 that, while young Treg cells efficiently suppressed Tconv cell proliferation, aged Treg  
122 cells were inferior in doing so (**Fig. 2A**). In addition, less Foxp3<sup>+</sup> aged Treg cells than  
123 young Treg cells were recovered in the culture (**Fig. 2B**), consistent with the impaired  
124 proliferative capacity of the aged Treg cells (**Fig. 1A and Fig. S1, E, G and H**). Next, we  
125 analyzed the Treg cell function *in vivo* by using naïve CD4 T cell induced colitis model  
126 (30) (**Fig. 2C**). Similar to what was observed *in vitro*, aged Treg cells failed to protect  
127 mice from naïve T cell elicited colitis compared to young Treg cells (**Fig. 2D**). Our  
128 unbiased genome-wide RNA-seq analysis revealed that aged Treg cells expressed normal  
129 levels of Treg signature genes (*Foxp3*, *Tnfrsf18* encoding GITR, *Ikzf2*, *Il2ra*, *Capg*) and  
130 increased expression of key inflammatory cytokines (*Il1a*, *Il1b*, *Il4*, *Il6*, *Il17a*, *Il17f*),  
131 while the expression of B7 receptor family members, chemokine receptors and Bcl2  
132 family members were not uniformly changed in aged Treg cells (**Fig. S2A**). This result  
133 indicates that ageing re-programs Treg cell function via multiple mechanisms to

134 contribute to their reduced expansion *in vitro* (**Fig. 2B**) and *in vivo* (**Fig. 2E and Fig.**  
135 **S2B**) and decreased survival (**Fig. S2C**).

136         Based on the results above, we hypothesized that Treg cells can restrain  
137 immunological ageing and such an ability of Treg cells declines when they age. To test  
138 this, we adopted an irradiation-induced immunological ageing model (31) to compare the  
139 ability of young and aged Treg cells to inhibit Tconv cell ageing (**Fig. 2F**). Low-dose  
140 irradiation effectively reduced naïve T cell population (**Fig. 2G left**) and induced Tconv  
141 cell ageing marked by *p16<sup>Ink4a</sup>* upregulation (**Fig. 2G right**), resembling immunological  
142 ageing. While the transferred young Treg cells could efficiently inhibit the Tconv cell  
143 ageing phenotype, aged Treg cells were inferior in doing so (**Fig. 2G**) and were poorly  
144 maintained in the periphery (**Fig. 2H**). Taken together, compared to Tconv cells, Treg  
145 cells are more prone to ageing and function deterioration.

146

#### 147 **DCAF1 deletion led to T cell ageing in young mice.**

148         We next explored the potential factors that control Treg cell ageing and found that  
149 the protein expression of DCAF1, a factor downregulated in the ageing tissues (32) (**Fig.**  
150 **S3A**), was also reduced in aged Treg cells (**Fig. 3A**). DCAF1 could be of interest because  
151 it is targeted by HIV (33) and controls p53 function (34), both of which contribute to  
152 immunological ageing (35-37). We deleted DCAF1 specifically in T cells in  
153 *Cd4Cre;Dcaf1<sup>fl/fl</sup>* mice (34). DCAF1 deletion in T cells led to elevated SA- $\beta$ -gal activity  
154 in both Treg cells and Tconv cells even in young *Cd4Cre;Dcaf1<sup>fl/fl</sup>* mice, with the highest  
155 SA- $\beta$ -gal activity observed in Treg cells (**Fig. 3B**). Heatmap and Pearson's correlation  
156 analysis of RNA-seq datasets revealed that *Dcaf1*-deficient Treg cells in young mice



157 adopted an expression profile similar to wild-type aged Treg cells when compared to  
158 young Treg (**Fig. 3C**). In addition, while DCAF1 deletion led to a global upregulation of  
159 ageing-related program and senescence signature genes in both Tconv and Treg cells  
160 (**Fig. 3D**), such an ageing phenotype appeared more pronounced in Treg cells (**Fig. 3E**).  
161 Therefore, DCAF1 is essential to restrict the ageing program of T cells and particularly  
162 Treg cells.

163

#### 164 **DCAF1 is required to restrain Treg cell ageing.**

165 Because T cell homeostasis of *Cd4Cre;Dcaf1<sup>fl/fl</sup>* mice was perturbed (34), the  
166 Treg cell phenotype observed in these mice could be confounded by the defects in Dcaf1-  
167 deficient Tconv cells. To investigate DCAF1 function in Treg cells specifically, we bred  
168 *Dcaf1<sup>fl/fl</sup>* mice with *Foxp3-EGFP-Cre* (FGC) mice to delete DCAF1 exclusively in Treg  
169 cells in *FGC;Dcaf1<sup>fl/fl</sup>* mice (**Fig. S3B**). Even though Treg cell population appeared not  
170 affected (**Fig. S3C**), the function of Treg cells was impaired as Tconv cells displayed  
171 activated phenotypes including increased effector/memory T cell populations and  
172 aberrant cytokine production in young *FGC;Dcaf1<sup>fl/fl</sup>* mice (**Fig. 4, A-D**), a phenotype  
173 similar to those in aged mice and *Cd4Cre;Dcaf1<sup>fl/fl</sup>* mice. Additionally, *FGC;Dcaf1<sup>fl/fl</sup>*  
174 mice ultimately developed splenomegaly and autoimmunity at the age of seven months  
175 (**Fig. 4, E and F**). Compared to wild-type Treg cells, Dcaf1-deficient Treg cells  
176 expressed similar levels of Treg signature genes (*Foxp3*, *Tnfrsf18* encoding GITR, *Ikzf2*,  
177 *Il2ra*, *Capg*) and increased expression of key inflammatory cytokines (*Il1a*, *Il1b*, *Il4*, *Il6*,  
178 *Il17a*, *Il17f*) (**Fig. S3D**), which was similar to that of aged Treg cells. Yet, they were  
179 defective in suppressing Tconv cell proliferation with impaired expansion (**Fig. 4G**) and

180 reduced proliferative capacity (**Fig. S3, E and F**) and survival (**Fig. S3G**). Consistent  
181 with what was observed in *Cd4Cre;Dcaf1<sup>fl/fl</sup>* mice, *FGC;Dcaf1<sup>fl/fl</sup>* Treg cells also adopted  
182 an ageing phenotype with elevated expression of senescence signature genes (**Fig. 4H**),  
183 indicating a Treg cell intrinsic role of DCAF1 in restraining Treg cell ageing.

184

### 185 **Treg cell ageing co-opts inflammation to promote immunological ageing.**

186 We noticed that Tconv cells in young *FGC;Dcaf1<sup>fl/fl</sup>* mice acquired an ageing  
187 phenotype (**Fig. 4H**), although they expressed normal levels of DCAF1 (**Fig. S3B**). This  
188 result suggested that the aberrant inflammation resulted from Treg cell ageing and  
189 functional deterioration could promote T cell ageing through cell-extrinsic mechanisms.  
190 To test this, we generated the mixed-bone-marrow chimeras where *FGC;Dcaf1<sup>fl/fl</sup>* and  
191 *FGC;Dcaf1<sup>fl/+</sup>* T cells co-existed in the same hosts (**Fig. 5A**). The presence of Dcaf1-  
192 sufficient Treg cells in mixed-bone-marrow chimeras suppressed T cell activation and  
193 cytokine production (**Fig. 5, B-E**) and prevented Tconv cells from acquiring ageing  
194 phenotype (**Fig. 5F**). Nonetheless, the ageing phenotype of Dcaf1-deficiency Treg cells  
195 persisted (**Fig. 5F**). Consistently, Dcaf1-deficient Treg cells remained inferior in  
196 populating the periphery than the co-existing wild-type Treg cells in the mixed-bone-  
197 marrow chimeras (**Fig. 5G**). Taken together with the results in Figure 4, these findings  
198 not only re-affirm a critical role for DCAF1 in restraining Treg cell ageing, but also  
199 suggest that Treg cell ageing and function deterioration may cause uncontrolled Tconv  
200 cell activation, inflammation, and immunological ageing.

201 **DCAF1 is required to restrain the ageing of human T cells**

202 While it has been documented that T and Treg cells in HIV patients display  
203 premature aging phenotypes (35, 36, 38, 39), the molecular mechanisms remain to be  
204 elucidated. To investigate whether DCAF1 is critical to prevent human T cell ageing, we  
205 utilized *Dcaf1* shRNA lentivirus to knockdown DCAF1 expression and examined the  
206 ageing phenotypes in human T cells. We designed two different shRNA constructs to  
207 efficiently downregulate DCAF1 expression in human T cells (**Fig. 6A**). We found that  
208 shRNA-mediated DCAF1 knockdown led to increased ROS level (**Fig. 6B**), increased  
209 SA- $\beta$ -gal activity in human T cells (**Fig. 6C**), and increased expression of ageing-related  
210 genes including *p16<sup>Ink4a</sup>* (**Fig. 6D**). Therefore, DCAF1 is important to prevent human T  
211 cell ageing, indicating that HIV infection may cause the premature ageing of human T  
212 cells by interfering with DCAF1.

213

214 **DCAF1 is required to suppress aberrant ERK activation during ageing.**

215 Intrigued by the above-mentioned findings, we further investigated the molecular  
216 mechanisms underlying Treg cell ageing. We found both aged Treg cells (**Fig. S4A**) and  
217 young *Dcaf1*-deficient Treg cells (**Fig. S4B**) paradoxically had a drastic ERK activation  
218 that normally promotes cell proliferation (40), despite their poor proliferative capacity.  
219 Such an ERK activation was not due to enhanced IL-2 signaling, because IL-2 activated  
220 STAT5 was reduced in these Treg cells (**Fig. S4, C and D**). The activation of ERK-Jun-  
221 p38 MAPK was reported in aged T cells from old humans (>65 years) and mice (16-20  
222 months old) (41). Yet, the upstream stimuli remain unclearly defined. By utilizing the  
223 tamoxifen-inducible-Cre (*ERCre*) mice (42), we were able to delete DCAF1 in

224 *ERCre;Dcaf1<sup>fl/fl</sup>* T cells acutely upon 4-hydroxy-tamoxifen treatment and analyze the  
225 causal effect of acute DCAF1 deletion. We found DCAF1 was critical to restrict such  
226 ERK activation because acute deletion of DCAF1 in activated T cells led to ERK  
227 activation (**Fig. S4E**), and the upregulation of critical ageing gene *p16<sup>Ink4a</sup>* (**Fig. S4F**).  
228 Importantly, interfering with the ERK activation attenuated the upregulation of *p16<sup>Ink4a</sup>* in  
229 Dcaf1-deficient T cells (**Fig. S4, G and H**). Thus, the observed ERK activation is  
230 important to promote T cell ageing (43) in a DCAF1 dependent manner.

231

### 232 **DCAF1 controls ROS accumulation, ERK activation and Treg cell ageing through** 233 **GSTP1.**

234 We next explored the pathways contributing to aberrant ERK activation and  
235 ageing in aged and Dcaf1-deficient Treg cells. Unbiased genome-wide RNA-seq analysis  
236 revealed ROS-pathway, which is known to cause ERK activation was upregulated and  
237 enriched in both aged Treg cells and young Dcaf1-deficient Treg cells (**Fig. 7, A and B**).  
238 Although appropriate level of ROS is important for T cell function (44), excessive ROS  
239 is a predominant contributor of cellular senescence and ageing (45, 46). We found ROS  
240 level was significantly elevated in both aged and Dcaf1-deficient Treg and Tconv cells  
241 (**Fig. 7, C and D**). Additionally, acute deletion of DCAF1 in *ERCre;Dcaf1<sup>fl/fl</sup>* T cells led  
242 to a prompt ROS upregulation in T cells (**Fig. 7E**), preceding ERK activation (**Fig. S4E**)  
243 and the upregulation of the ageing signature gene *p16<sup>Ink4a</sup>* (**Fig. S4F**). These results  
244 suggest that the excessive ROS contributed to ERK activation and ageing in both aged  
245 and Dcaf1-deficient Treg cells.

246 To study how DCAF1 regulates ROS, we analyzed DCAF1 interactome from two  
247 independent immunoprecipitation-mass spectrometry (IP-MS) experiments using both T  
248 and non-T cells (34, 47). While DCAF1-regulated pathways, including DNA repair, cell  
249 cycle arrest and unfolded protein response, could indirectly induce ROS (**Fig. S5, A and**  
250 **B**), DCAF1 was found bound to GSTP1, which was further validated by co-  
251 immunoprecipitation assays both in 293T cell and endogenous immunoprecipitation in  
252 mouse T cells (**Fig. 7, F and G**). GSTP1 is one of the glutathione S-transferase (GST)  
253 family members that catalyze intracellular detoxification reactions by conjugating  
254 glutathione with hydrophobic and electrophilic compounds (48). Depletion of Gstp1 or  
255 pharmacological inhibition of its activity increases ROS level and ERK phosphorylation  
256 (49). Overexpression of Gstp2 (a Gstp1 orthologue in *C. elegans*) enhanced stress  
257 resistance and extended lifespan in *C. elegans* (50). Given the known function of DCAF1  
258 as a component of an E3 ubiquitin ligase complex to not only regulate protein  
259 degradation via polyubiquitylation but also regulate protein function via mono-  
260 ubiquitylation (47), we investigated if DCAF1 regulated the ubiquitylation of GSTP1.  
261 We found that GSTP1 was mono-ubiquitinated and DCAF1 promoted mono-  
262 ubiquitylation but not poly-ubiquitylation of GSTP1 (**Fig. S5C**). It suggests that DCAF1  
263 may facilitate GSTP1 function. Indeed, we found that the expression of GSTP1 promoted  
264 glutathione S-transferases activity and the co-expression of DCAF1 further enhanced its  
265 glutathione S-transferases activity (**Fig. 7H**). In agreement, glutathione S-transferases  
266 activity was significantly downregulated in both aged and Dcaf1-deficient Treg cells  
267 (**Fig. S5, D and E**). Additionally, knockdown of DCAF1 in human T cells led to  
268 decreased glutathione S-transferases activity (**Fig. S5F**). Next, we overexpressed GSTP1

269 in Dcaf1-deficient T cells and found overexpression of Gstp1 suppressed the excessive  
270 ROS accumulation (**Fig. 7I**) and ERK phosphorylation (**Fig. S6A**) in Dcaf1-deficient T  
271 cells. Importantly, overexpression of GSTP1 corrected the proliferation defects of aged  
272 Treg cells (**Fig. 7J**). These findings suggest that DCAF1 promotes the function of GSTP1  
273 via mono-ubiquitylation to restrain ROS accumulation and Treg cell ageing.

274

### 275 **Suppression of ROS reinvigorates the proliferation and function of aged Treg cells**

276 Multiple strategies have been developed to delay and even reverse the aging  
277 process (9). As ROS is a predominant contributor of cellular senescence and ageing (45,  
278 46), we next wondered if targeting excessive ROS could suppress Treg cell ageing and  
279 rejuvenate the suppressive function of aged Treg cells. By using ROS scavengers  
280 including N-acetyl-L-cysteine (NAC) and Glutathione (GSH), we can effectively  
281 downregulate ROS level in both aged and Dcaf1-deficient Treg cells (**Fig. 8, A and B**).  
282 Interestingly, suppression of excessive ROS also drastically promoted the proliferation of  
283 both aged and Dcaf1-deficient Treg cells (**Fig. 8, C and D**). Next we analyzed the effect  
284 of ROS scavengers on the function of aged and Dcaf1-deficient Treg cells by in vitro  
285 suppression assay. To avoid the effects of NAC/GSH on responder T cells, we pretreated  
286 Treg cells with N-acetyl-L-cysteine (NAC) and Glutathione (GSH) for 24 hours before  
287 adding them into co-culture for Treg suppression assay. We found ROS scavenger  
288 treatment was effective in reinvigorating the immune suppression function of aged and  
289 Dcaf1-deficient Treg cells (**Fig. 8, E and F**). Taken together, these findings demonstrate  
290 that excessive ROS is a critical mechanism underlying Treg cell ageing and functional  
291 deterioration during immunological ageing.

292 **Discussion**

293 Ageing and age-associated diseases have become the pressing health issues  
294 world-wide (2). The immune system is greatly impacted by ageing, displaying chronic  
295 inflammation (inflammageing) and declined immune function (immunosenescence)  
296 during ageing. Thus, understanding the cellular and molecular mechanisms underlying  
297 the alterations of immune regulation during ageing is vital to find ways to address age  
298 related health issues. This study investigated whether and how the function of Treg cells  
299 is regulated during immunological ageing. By combining comprehensive *in vitro* and *in*  
300 *vivo* approaches, we showed an unexpected cell-intrinsic propensity of Treg cells to  
301 preferentially senesce over Tconv cells through DCAF1-GSTP1-ROS-dependent  
302 mechanisms, causing an increasing imbalance between the function of Treg and Tconv  
303 cells during ageing to favor Tconv cell activation and inflammation, which in turn further  
304 promotes immunological ageing (**Fig. S7**). Our findings support the notion that Treg cells  
305 play critical roles in restraining immunological ageing and offer potential molecular  
306 targets, such as GSTP1-ROS axis, for reinvigorating Treg cell function during ageing.

307 Treg cell population has been found elevated in lymphoid tissues during  
308 immunological ageing in both human and mouse studies consistently (18, 20, 23). It is  
309 intuitive to believe that such Treg cell increase leads to increased immune suppression.  
310 Early studies suggested that the function of aged Treg cells was unchanged or increased  
311 based on *in vitro* experiments using bulk T cells without specifically investigate the  
312 intrinsic function of Treg cells (17-19). While these findings appear to explain certain  
313 age-related conditions including higher incidence of tumor development, which could  
314 also be driven by ageing related chronic inflammation (51), they contradict the

315 observation that immunological ageing is marked by a low grade, chronic systemic  
316 inflammation with accumulation of effector-memory T cells and is also associated with  
317 high incidence of autoimmunity (52). Moreover, emerging evidence indicates that aged  
318 Treg cells may be functionally defective *in vivo* (20, 21). The discrepancy could be due  
319 to the difference in the assays used. In the studies using <sup>3</sup>H-thymidine incorporation  
320 assay to assess Treg cell suppression, the proliferative capacity of responder T cells and  
321 Treg cells could not be distinguished. Therefore a decrease in <sup>3</sup>H-thymidine could be due  
322 to reduced proliferation of responder T cells, Treg cells or both. Thus, the results of <sup>3</sup>H-  
323 thymidine incorporation assay are not only determined by responder T cell proliferation,  
324 but also confounded by co-existing Treg cells. Therefore, the results of Treg cell  
325 suppression assayed by <sup>3</sup>H-thymidine incorporation may vary substantially and  
326 conflicting results of how well aged Treg cells suppress are indeed reported (20, 27). To  
327 specifically assess the proliferation of Treg cells and responder T cells, we distinguished  
328 them by their expression of different congenic markers (CD45.1 vs. CD45.2). Using this  
329 method, we found that young Treg cells proliferated substantially to contribute to <sup>3</sup>H-  
330 thymidine incorporation of total cell culture. Yet, aged Treg cells proliferated much less,  
331 which may contribute to the reduced <sup>3</sup>H-thymidine incorporation of total cell culture.  
332 Taken together with results from the colitis model and irradiation induced ageing model,  
333 our study demonstrated that aged Treg cells manifested exacerbated ageing to contribute  
334 to deteriorated proliferation in response to activation *in vitro* and *in vivo* and were inferior  
335 in suppressing Tconv cell activation during ageing. These findings therefore shed light on  
336 the long-sought mechanisms underlying age-associated chronic inflammation that  
337 contributes to age-related morbidities.



338 Accelerated T cell senescence is found in AIDS patients even after anti-retroviral  
339 therapy (35, 36) to contribute to the high mortality rate of AIDS patients despite active  
340 HIV infection is under control (53). We found that DCAF1, a HIV-1 virus cellular target  
341 that is downregulated during ageing, was essential to restrain T cell, especially Treg cell,  
342 ageing. In addition, inflammation resulting from defective Treg cell function promoted T  
343 cell ageing. These findings suggest that HIV may promote T cell attrition in AIDS  
344 patients through two mutually related mechanisms. One is to target DCAF1 to directly  
345 induce T cell ageing. The other is to trigger Treg cell ageing to induce chronic  
346 inflammation, which in turn exacerbates the ageing program of T cells for reduced  
347 function. It presents an interesting possibility that, by restoring DCAF1 function and by  
348 reinvigorating Treg cell function, we may reduce systemic inflammation and T cell  
349 attrition to benefit AIDS patients. Therefore, further study of the underlying mechanisms  
350 of DCAF1 downregulation during ageing will not only benefit ageing-related diseases,  
351 but also provide a potential means to reduce immune senescence in AIDS patients.

352 The cellular level of ROS is subject to tight redox regulation, and disruption of  
353 the ROS balance may lead to excessive ROS causing cellular senescence and ageing (45,  
354 46). Here we found ROS level was preferentially increased in Treg cells compared to  
355 Tconv cells regardless of age, which agrees with the previous finding that ROS is  
356 required for the suppressive function of Treg cells (54). We found the excessive ROS  
357 impaired the proliferative capacity and function of aged Treg cells, and ROS scavenging  
358 agents reinvigorated the proliferation and suppressive function of aged T cells. By using  
359 IP-MS-based DCAF1 interactome analysis, we identified one of the potential  
360 mechanisms, where DCAF1 regulated ROS through GSTP1-mediated ROS

361 detoxification. Given the emerging role of glutathione in buffering ROS and regulating  
362 multiple processes in T cells (55), further studies on the detailed mechanisms of DCAF1-  
363 GSTP1 axis in regulating glutathione mediated detoxification pathway will provide  
364 valuable insights not only in immunological ageing, but also in the general function of  
365 immune cells. Additionally, we found that many pathways regulating cellular ROS  
366 generation (56) including PI3K-Akt-mTOR, DNA damage-p53 response and  
367 inflammation, were altered in aged Treg cells. Therefore, both ROS generation and  
368 detoxification appear to be involved in controlling the function of aged Treg cells. Of  
369 interest, the inhibition of mTOR signaling pathway has been associated with healthier  
370 ageing and longevity, especially for the hematopoietic system (57), which suggests that  
371 PI3K-Akt-mTOR may be particularly important for Treg cell ageing. It therefore  
372 warrants further investigation if targeting mTOR may also ameliorate Treg cell ageing  
373 and inflammation through reducing ROS. In addition, because the current study  
374 highlights a critical role for ROS in Treg cell ageing, it proposes that targeting ROS may  
375 be a viable approach to rejuvenate Treg cells to mitigate immunological ageing.  
376 Therefore, further in-depth studies of ROS-related pathways in regulating Treg cell  
377 ageing may shed new light on the precise mechanisms underlying immunological ageing  
378 and to reveal potential targets to mitigate adversary effects of inflamm-ageing with the  
379 aim of improving the health of the ageing population.

## 380 **Materials and Methods**

### 381 **Animals**

382 *Rag1*<sup>-/-</sup>, Foxp3-GFP-Cre (FGC) and CD45.1 congenic wild-type (WT) mice were  
383 purchased from Jackson laboratory and maintained on C57BL/6 background. *Dcaf1*<sup>fl/fl</sup>

384 (58), *Cd4Cre* (59), and *ERCre* (42) mice were on C57BL/6 background as reported  
385 previously. Aged wild-type (WT) mice (>18 months old) were either from retired breeder  
386 or from National Institute on Ageing (NIA). All mice were housed and bred under  
387 specific pathogen free conditions in the animal facility at the University of North  
388 Carolina at Chapel Hill.

### 389 **Lymphocyte isolation, antibody staining, flow cytometry and cell sorting**

390 Lymphocytes were isolated from various lymphoid organs of mice of indicated  
391 age and genotype. Fluorescence-conjugated antibodies for CD4 (GK1.5), CD8 (53-6.7),  
392 CD45.1 (A20), CD45.2 (104), CD45RB (C363-16A), CD25 (PC61.5), CD44 (IM7),  
393 CD62L (MEL-14), anti-IFN $\gamma$  (XMG1.2), and anti-IL4 (11B11) were purchased from  
394 Biolegend. The anti-Foxp3 antibody (FJK-16s) and Foxp3 staining kit (00-5523-00)  
395 were purchased from eBioscience. Annexin V (BD Bioscience, 550474) and 7AAD (BD  
396 Bioscience, 559925) staining were used to assess apoptosis per manufacturer's protocols.  
397 For intracellular cytokine staining, lymphocytes were stimulated for 4 hours with 50  
398 ng/mL of PMA (phorbol 12-myristate 13-acetate) and 1  $\mu$ M ionomycin in the presence of  
399 brefeldin A. The cells were stained with antibodies against surface markers and then  
400 fixed and permeabilized with a commercially available kit (BD Biosciences) for  
401 intracellular cytokine staining per the manufacturer's protocol. The stained cells were  
402 analyzed on LSRFortessa station (BD Biosciences) or Canto (BD Biosciences).

403 For Treg cell sorting, CD25<sup>+</sup> T cells were firstly stained by anti-CD25 biotin  
404 antibody and enriched by Streptavidin MicroBeads (Miltenyi Biotec) and then stained  
405 with anti-CD4 and anti-CD25 fluorescence-conjugated antibodies. For CD4 T cell  
406 sorting, CD4<sup>+</sup> T cells were enriched by MACS beads (Miltenyi Biotec) and then stained

407 with fluorescence-conjugated antibodies. Stained cells were washed and sorted on the  
408 Moflow cell sorter (Dako cytometry, Beckman Coulter) by the flow facility of the  
409 University of North Carolina at Chapel Hill.

410 For detecting SA- $\beta$ -gal activity in T cells with the fluorescent  $\beta$ -galactosidase  
411 substrate C<sub>12</sub>FDG: The assay was adopted from previously published protocol (60).  
412 Freshly isolated lymphocytes were pretreated with 100 nM Bafilomycin A1 (Sigma,  
413 B1793) for 1 hour before adding 33  $\mu$ M of C<sub>12</sub>FDG (Sigma, F2756) for additional 2  
414 hours in 37 °C incubator. The cells were harvested and washed in cold 1 X PBS for three  
415 times before staining with antibodies for FACS analysis.

416 For detecting ROS level in T cells: The DCFDA assay for detecting ROS was  
417 used as described previously (61). Freshly isolated lymphocytes or cultured T cells were  
418 stained with antibodies firstly. After staining, the cells were washed by 1 X PBS and  
419 seeded in pre-warmed medium in 24-well plate. A final concentration of 2  $\mu$ M of  
420 DCFDA (Sigma, D6883) was added. Cells were cultured for 20 minutes and then  
421 harvested and washed with cold 1X PBS followed by flow-cytometry. All the FACS data  
422 were analyzed with FlowJo software (TreeStar).

### 423 ***In vitro* T cell culture, activation and proliferation**

424 To assess Treg cell proliferation *in vitro*, 1 x 10<sup>4</sup> Treg cells from young mice  
425 (CD45.1) and 1 x 10<sup>4</sup> Treg cells from aged mice (CD45.2) were cocultured with 1 x 10<sup>5</sup>  
426 naive CD4 T cells from young mice in the presence of soluble CD3 antibody (Bio X Cell,  
427 2C11, 1  $\mu$ g/ml) and 4 x 10<sup>5</sup> irradiated (3000 cGy) T cell-depleted splenocytes in RPMI  
428 1640 medium containing 10% FBS, 1% penicillin-streptomycin and 2.6  $\mu$ l of  $\beta$ -  
429 Mercaptoethanol. Cell proliferation was assessed by CFSE (carboxyfluorescein

430 succinimidyl ester) dilution assay or BrdU (5-bromo-2'-deoxyuridine) incorporation  
431 assay at indicated time points post activation.

432 For CFSE dilution assay, T cells were labeled in 2  $\mu$ M CFSE (Life Technologies,  
433 C1157) and cultured in the presence of 2 ng/ml IL-2. For BrdU incorporation assay,  
434 cultured T cells were pulsed with BrdU for one hour prior to harvest, stained with BrdU  
435 staining kit per manufacture's protocols (BD Pharmingen, 559619) and analyzed by flow-  
436 cytometry. To inhibit ERK phosphorylation, MEK inhibitor (PD98095) was added during  
437 T cells activation at a final concentration of 50  $\mu$ M. For assays with ROS scavengers,  
438 stock solution of 0.5 M NAC (N-acetyl-cysteine, Sigma, A9165) and 0.3 M GSH  
439 (Glutathione, VWR IC10181405) were prepared in ddH<sub>2</sub>O and adjusted to pH 7.0 with  
440 10 N NaOH. A final concentration of 20 mM of NAC and 10 mM of GSH was added to  
441 cell culture as indicated in experiment.

#### 442 ***In vitro* Treg suppression assay**

443 CD4<sup>+</sup>CD25<sup>-</sup>CD62L<sup>+</sup>CD44<sup>-</sup> naïve T cells (responder) from young WT mice  
444 (CD45.1) and CD4<sup>+</sup>CD25<sup>+</sup> Treg cells (suppressor) from young WT mice (CD45.2), aged  
445 WT mice (CD45.2) and young *FGC;Dcaf1<sup>fl/fl</sup>* mice (CD45.2) were sorted by FACS.

446 To assess the efficacy of Treg cell-mediated immune suppression *in vitro*, 1 x 10<sup>5</sup>  
447 sorted responder T cells from young WT mice were labeled with CFSE and mixed with  
448 varying amounts (as indicated) of Treg suppressor cells. Cell mixtures were stimulated  
449 with soluble anti-CD3 (Bio X Cell, 2C11, 0.125  $\mu$ g/ml) in the presence of 4 x 10<sup>5</sup>  
450 irradiated (3000 cGy) T cell-depleted splenocytes. The proliferation of responder cells  
451 was assessed by CFSE dilution detected by flow-cytometry 72 hr after activation.

452 To assess the effect of ROS scavengers on Treg suppression, Treg cells were

453 pretreated with 20 mM of NAC or 10 mM of GSH for 24 hours in the presence of anti-  
454 CD3 (Bio X Cell, 2C11, 5 µg/ml) and anti-CD28 (Bio X Cell, 35.51, 2 µg/ml) antibodies  
455 and IL-2 (500 U/ml). Treg cells were washed with RPMI164 medium to remove residual  
456 ROS scavengers before used for *in vitro* suppression assay.

#### 457 **Human T cell purification, activation and culture**

458 For human T cell studies, CD4<sup>+</sup> T cells were purified by human CD4 isolation kit  
459 (MACS, Order no. 130-096-533) from human buffy coat obtained from Gulf Coast  
460 Regional Blood Center. Purified CD4<sup>+</sup> T cells were cultured in RPMI 1640 medium  
461 containing 10% FBS, 1% penicillin-streptomycin and 2.6 µl of β-Mercaptoethanol and  
462 activated with anti-CD3/CD28 stimulator (Stem cell, Cat # 10971) in the presence of  
463 human IL-2 (100 U/ml).

#### 464 **shRNA-mediated DCAF1 knockdown in human T cells**

465 Human *Dcaf1* shRNA lentivirus production: The human *Dcaf1* shRNA in  
466 lentivirus vector was from the RNAi Consortium, with shRNA1 (TRCN0000129831)  
467 targeting GCGCCAATAAACTTTACGTCA and shRNA2 (TRCN0000130734) targeting  
468 GCGCCAATAAACTTTACGTCA. HEK293T cells (ATCC) were transfected with 3 µg  
469 of shRNA plasmids, 3 µg of packaging plasmids (1 µg of psPAX2, 2 µg of pMD2.G)  
470 using FuGENE® 6 (Promega) transfection reagent. After 48 hours, viruses were  
471 harvested, filtered through 0.45 µm syringe filters and stocked in -80° C freezers.

472 For transduction of human T cells, human CD4<sup>+</sup> T cells were purified and  
473 activated with anti-CD3/anti-CD28 beads for 48 hours and then transduced with  
474 lentivirus encoding *Dcaf1* shRNA or scrambled control with 8 µg/ml polybrene (Sigma-

475 Aldrich) by centrifuge at 1500 g for 120 minutes. Puromycin (2 µg/mL) was added for  
476 the selection of transduced cells after 48 hours of transduction. Cells were harvested 4  
477 days post transduction for ROS analysis and 6 days post transduction for aging marker  
478 analysis.

#### 479 **Treg cell-mediated protection of naive CD4 T cell-elicited colitis *in vivo***

480 1 x 10<sup>5</sup> sorted Treg cells from either young or aged mice (CD45.2) were mixed  
481 with 2 x 10<sup>5</sup> naive (CD4<sup>+</sup>CD25<sup>-</sup>CD45RB<sup>hi</sup>) T cells sorted from wild-type young mice  
482 (CD45.1). Cell mixture was transferred into *Rag1*<sup>-/-</sup> mice. As a control, 2 x 10<sup>5</sup> naive  
483 CD4<sup>+</sup> T cells were transferred alone. To monitor the colitis development, body weight of  
484 the recipient mice was measured weekly after the transfer. T cells from these mice were  
485 harvested and subjected to immunological analysis at the end of the experiments.

#### 486 **Generation of mixed bone marrow chimera**

487 Bone marrow cells were isolated from age- and gender-matched *FGC;Dcaf1*<sup>fl/fl</sup>  
488 (CD45.2) and *FGC;Dcaf1*<sup>fl/+</sup> (CD45.1.2) littermates, mixed at a ratio of 1:1 and  
489 transferred into sub-lethally irradiated (500 cGy) *Rag1*<sup>-/-</sup> mice. T cells in the reconstituted  
490 recipients were analyzed 8-10 weeks post transfer.

#### 491 **Suppression of irradiation induced Tconv ageing by Treg cells *in vivo***

492 The assays to induce T cell ageing by irradiation were adopted from a previously  
493 publication (31). Young WT mice (CD45.1) were sub-lethally irradiated (400 cGy). 2 x  
494 10<sup>6</sup> Treg cells isolated from either young or aged mice (CD45.2) were transferred into  
495 irradiated mice. Different time points after transfer, T cell populations in the irradiated  
496 mice with or without Treg cell transfer were analyzed.

497 **RNA preparation, qRT-PCR and RNA-Seq**

498 Total RNA was prepared from T cells using TRIzol reagent (Invitrogen) per  
499 manufacturer's instructions and was reverse-transcribed into cDNA with iScript™ cDNA  
500 Synthesis Kit (BioRad). Quantitative PCR was performed on ABI9700 real-time PCR  
501 system with Taqman-probe sets purchased from Applied Biosystems and Integrated DNA  
502 Technologies (IDT).

503 For the human T cell study, the gene expression was analyzed by SYBR Green  
504 assay. The primers of *p16<sup>Ink4a</sup>* (Forward: CTCGTGCTGATGCTACTGAGGA; Reverse:  
505 GGTCGGCGCAGTTGGGCTCC, Cat#: HP226191) and *β-actin* (Forward:  
506 CACCATTGGCAATGAGCGGTTC; Reverse: AGGTCTTTGCGGATGTCCACGT;  
507 Cat #: HP204660) were designed by Origene.

508 For RNA-seq analysis, total RNA was extracted from T cells by using RNA-easy  
509 mini kit (Qiagen). RNA-seq libraries were generated and poly(A) enriched with 1  
510 microgram of RNA as input using the TruSeq RNA Sample Prep Kit (Illumina, San  
511 Diego, CA). Indexed samples were sequenced using the 50bp paired-end protocol via the  
512 HiSeq 2500 (Illumina) per the manufacturer's protocol. Reads (30-46 Million reads per  
513 sample) were analyzed with Salmon (version 0.9.1) software (62) to align and quantify  
514 the transcript expression. R packages in Bioconductor, tximport and tximportData (63)  
515 were used to aggregate transcript-level quantifications to the gene level, with the R  
516 package biomaRt for gene and transcripts mapping.

517 The option "lengthScaledTPM" for countsFromAbundance in tximport was used  
518 to obtain the estimated counts at the gene level using abundance estimates scaled based  
519 on the average transcript length over samples and the library size. For the differential



520 expression (DE) analysis of RNA-seq data, gene-level count matrix was passed into  
521 DESeq2 package (64) as input directly from the tximport package. Based on the  
522  $\log_2(\text{FC}) > 1.5$ ,  $\text{padj} < 0.05$  criteria, 863 genes were differentially regulated in old treg cells  
523 compared to their young counterparts. The normalized gene expression data was retrieved  
524 from DESeq2 analysis after regulated log (rlog) transformation ('rlog' in DESeq2)(64).  
525 The z-score at gene-level average of normalized expression matrix was used to generate  
526 heatmap in Gene-E from Broad Institute ([www.broadinstitute.org/ /GENE-E/](http://www.broadinstitute.org/GENE-E/)).

527 Gene Set Enrichment Analysis (65) was performed using the Java application  
528 available from Broad Institute ([www.broadinstitute.org/gsea/](http://www.broadinstitute.org/gsea/)). Gene set databases  
529 including Hallmarks ([h.all.v6.1.symbols.gmt](http://h.all.v6.1.symbols.gmt)) and KEGG ([c2.cp.kegg.v6.1.symbols.gmt](http://c2.cp.kegg.v6.1.symbols.gmt))  
530 from the Molecular Signatures Database (MSigDB) (66) were used in the analysis. The  
531 ageing-program gene set was from DEMAGALHAES\_AGEING\_UP (26) in MSigDB.  
532 One thousand gene set permutations were performed.  $\text{FDR} < 0.05$  was used for enriched  
533 terms, as is recommended when performing permutations by gene set.

534 R version 3.5.0 was used. The RNA-seq data are available in the Gene Expression  
535 Omnibus repository at the National Center for Biotechnology Information under  
536 accession number GSE130419.

### 537 **Immunoblotting and immunoprecipitation**

538 Cells were lysed in NP40 lysis buffer (1% Nonidet P-40, 50 mM Tris (pH 7.5),  
539 150 mM NaCl, 10% glycerol) containing protease inhibitor cocktail (Roche Molecular  
540 Biochemicals). The crude lysates were cleared by centrifugation at 14,000 rpm at 4°C for  
541 15 min. Cell lysate was treated with 2x Laemmli sample buffer (Bio-Rad, 1610737) and  
542 incubated at 95 °C for 5 minutes. Protein extracts were resolved by AnyKD SDS-PAGE

543 gel (Bio-Rad, 4569034) and transferred to a polyvinylidene fluoride (PVDF) membrane  
544 (Millipore) and analyzed by immuno-blotting with the following antibodies:  $\beta$ -actin,  
545 Santa Cruz (I-19), WB (1:2000); DCAF1, ProteinTech (11612-1-AP), WB (1:2000), IP  
546 (1:200); GSTP1, Invitrogen (PA5-29558), WB (1:1000); pan ERK, BD (610123), WB  
547 (1:2000); p-ERK, Cell Signaling (4370), WB (1:2000); total STAT5, Cell Signaling  
548 (9358), WB (1:2000); pSTAT5, Cell Signaling (4322), WB (1:2000).

549 For immunoprecipitation of endogenous DCAF1 and GSTP1 in mouse T cells,  
550 CD4 T cells were purified by MACS and activated by anti-CD3 and anti-CD28 for 24  
551 hours. The cells were treated with MG132 for 4 hours prior to harvest. Cells were lysed  
552 in NP40 lysis buffer (1% Nonidet P-40, 50 mM Tris (pH 7.5), 150 mM NaCl, 10%  
553 glycerol) containing protease inhibitor cocktail (Roche Molecular Biochemicals) and  
554 MG132 and crude lysates were cleared by centrifugation at 14,000 rpm at 4°C for 15 min.  
555 The soluble fraction was divided into two parts and incubated with magnetic beads that  
556 conjugated with DCAF1 antibody (ProteinTech, 11612-1-AP) or rabbit IgG in cold room  
557 overnight. The immunocomplex was washed four times with NP40 lysis buffer and then  
558 three times with PBS. Associated proteins were eluted by 2X Laemmli sample buffer  
559 (Bio-Rad, 1610737) and incubated at 95°C for 5 minutes. The eluted proteins were  
560 resolved in SDS-PAGE gel (Bio-Rad, 4569034). For immunoprecipitation of  
561 overexpressed DCAF1 and GSTP1 in 293T cells, the cell lysate from 293T cells  
562 transfected with pCDNA-Myc-Dcaf1 and MIT-Flag-Gstp1 plasmids was prepared and  
563 subjected to immunoprecipitation with FLAG® M2 beads (Sigma, M8823).

#### 564 **GSTP1 ubiquitylation assay**

565 For the GSTP1 ubiquitylation assay, 293T cells were transfected with plasmid of  
566 MYC-DCAF1, FLAG-GSTP1 and HA-Ubiquitin as indicated for 48 hours and treated  
567 with 100  $\mu$ M of proteasome inhibitor MG132 (Santa Cruz, sc-201270A) for additional 4  
568 hours before harvest. Lysates were prepared with NP40 lysis buffer, denatured in 1% of  
569 SDS and diluted 10 folds before immunoprecipitation. FLAG-GSTP1 was  
570 immunoprecipitated with anti-FLAG (Sigma, M2) antibody and analyzed by immunoblot  
571 with anti-HA (Roche, 3F10), anti-MYC (Sigma, 4A6) and anti-FLAG (Sigma, M2)  
572 antibodies as indicated.

### 573 **Glutathione S-transferase (GST) activity assay**

574 Glutathione S-transferase activity was analyzed by the increase of the absorbance  
575 at 340 nm at 25°C with reduced glutathione (GSH) and 1-chloro-2, 4-dinitrobenzene  
576 (CDNB) as substrates. The Glutathione S-Transferase (GST) Assay Kit (Sigma, CS0410)  
577 was used per manufacturer's protocols. Briefly, 1 million cells were lysed in 50  $\mu$ l of  
578 sample buffer by sonication. Then 30  $\mu$ l of the samples were added into the assay  
579 cocktail (150  $\mu$ l of PBS pH 6.5, 10  $\mu$ l of 100 mM CDNB and 10  $\mu$ l of 100 mM GSH) in  
580 96-well plate and immediately analyzed in a plate reader. The change in absorbance  
581 ( $\Delta A_{340}$ )/minute, in the linear range of the plot, using the following equation:

$$582 \quad (\Delta A_{340})/\text{min} = [A_{340}(\text{final read}) - A_{340}(\text{initial read})]/\text{reaction time (min)}$$

583 GST specific activity per million cells ( $\mu$ mol/million/min) were calculated using the  
584 following equation:

$$585 \quad [(\Delta A_{340})/\text{min} \times V(\text{ml}) \times \text{dilution}] / [\epsilon_{\text{mM}} \times V_{\text{enz}}(\text{ml}) \times \text{density}]$$

586 For our assay using 96-well plate:  $\epsilon_{\text{mM}} = 5.3 \text{ mM}^{-1}$ ;  $V(\text{ml}) = 0.2 \text{ ml}$ ;  $V_{\text{enz}}(\text{ml}) =$  the volume  
587 of the enzyme sample tested, density = number of cell used in cell lysate.

588 **Histology**

589 Tissues were resected and fixed in 4% formalin for one week, cleared with xylene  
590 and embedded in paraffin. Sections of 5  $\mu\text{m}$  thickness were collected and stained with  
591 Hematoxylin and Eosin (H&E). The sections were examined under a microscope and an  
592 aggregation of more than 50 mononuclear cells in the tissue marked lymphocytic  
593 infiltration.

594 **Statistical analysis**

595 Data analysis was performed and grafted by Prism (GraphPad, San Diego).  
596 Statistical significance was determined by Mann-Whitney's U test, two-tailed Student's *t*  
597 test, one-way ANOVA post Turkey's multiple comparisons test, and two-way ANOVA  
598 post Sidak's multiple comparisons test as indicated. A *p* value of less than 0.05  
599 (confidence interval of 95%) was considered significant. In the figures, asterisks are used  
600 to indicate *P* values as follows: ns, not significant,  $p > 0.05$ ,  $*p < 0.05$ ,  $**p < 0.01$ ,  $***p$   
601  $< 0.001$  and  $****p < 0.0001$ . The sample sizes (*n*) are stated in the figure legends to  
602 indicate biologically independent replicates used for statistical analysis.

603 **Data availability**

604 The RNA-seq data supporting the findings of this study have been deposited in  
605 the Gene Expression Omnibus at the National Center for Biotechnology Information  
606 under accession number GSE130419. The IP-MS proteomics data supporting the findings  
607 of this study have been deposited in the ProteomeXchange Consortium via the PRIDE  
608 partner repository with the dataset identifier PXD003180 (Ref. (34)). The published data  
609 for proteome changes during mouse brain ageing was from PXD005230 (Ref. (32)).

610 **Study approval**

611 All mouse experiments in this study were approved by Institutional Animal Care  
612 and Use Committee of the University of North Carolina at Chapel Hill.

613 **Acknowledgments:**

614 We thank Nancy Fisher and Janet Dow (UNC Flow-cytometry facility support in  
615 part by P30 CA016086 Cancer Center Core Support Grant) for cell sorting; Cheng Chris  
616 Fan (UNC) for bioinformatics analysis; Dr. Yue Xiong for providing *Dcaf1<sup>fl/fl</sup>* mice; Dr.  
617 Yuan Zhuang for critical reading of this manuscript. This study was supported by the  
618 NIH (R01-MH101819-01; P30ES010126) for D.W., by the NIH (R01-AI029564) and the  
619 National Multiple Sclerosis Society (CA10068) for J.P.-Y.T., and by the NIH  
620 (AI123193), the National Multiple Sclerosis Society (RG-1802-30483) for Y.Y.W..

621 **Author contributions:**

622 Z. G. designed and performed cellular, molecular, biochemical, bioinformatics  
623 and animal experiments, and wrote the manuscript. G.W. and J.Z. contributed to RNA-  
624 seq experiment. B.W. contributed to Treg cell proliferation experiments. W.C. and J.P.-  
625 Y.T. contributed to colitis experiments. L.C. and L.S. contributed to human T cell  
626 experiments. J.L. and D. W. contributed to bio-informatic analysis. C.Z. contributed  
627 critical reagents for ageing analysis. Y.Y.W. conceived the project, designed experiments  
628 and wrote the manuscript.

629 **Competing interests:**

630 The authors declare no competing interests.

631

632 **References and Notes:**

- 633 1. Fulop T, Larbi A, Dupuis G, Le Page A, Frost EH, Cohen AA, Witkowski JM,  
634 and Franceschi C. Immunosenescence and Inflamm-Aging As Two Sides of the  
635 Same Coin: Friends or Foes? *Frontiers in immunology*. 2017;8(1960).
- 636 2. Partridge L, Deelen J, and Slagboom PE. Facing up to the global challenges of  
637 ageing. *Nature*. 2018;561(7721):45-56.
- 638 3. Franceschi C, and Campisi J. Chronic inflammation (inflammaging) and its  
639 potential contribution to age-associated diseases. *The journals of gerontology*  
640 *Series A, Biological sciences and medical sciences*. 2014;69 Suppl 1(S4-9).
- 641 4. Kennedy BK, Berger SL, Brunet A, Campisi J, Cuervo AM, Epel ES, Franceschi  
642 C, Lithgow GJ, Morimoto RI, Pessin JE, et al. Geroscience: linking aging to  
643 chronic disease. *Cell*. 2014;159(4):709-13.
- 644 5. Ovadya Y, Landsberger T, Leins H, Vadai E, Gal H, Biran A, Yosef R, Sagiv A,  
645 Agrawal A, Shapira A, et al. Impaired immune surveillance accelerates  
646 accumulation of senescent cells and aging. *Nature communications*.  
647 2018;9(1):5435.
- 648 6. Furman D, Campisi J, Verdin E, Carrera-Bastos P, Targ S, Franceschi C, Ferrucci  
649 L, Gilroy DW, Fasano A, Miller GW, et al. Chronic inflammation in the etiology  
650 of disease across the life span. *Nat Med*. 2019;25(12):1822-32.
- 651 7. Milikovsky DZ, Ofer J, Senatorov VV, Jr., Friedman AR, Prager O, Sheintuch L,  
652 Elazari N, Veksler R, Zelig D, Weissberg I, et al. Paroxysmal slow cortical

- 653 activity in Alzheimer's disease and epilepsy is associated with blood-brain barrier  
654 dysfunction. *Science translational medicine*. 2019;11(521).
- 655 8. Senatorov VV, Jr., Friedman AR, Milikovsky DZ, Ofer J, Saar-Ashkenazy R,  
656 Charbash A, Jahan N, Chin G, Mihaly E, Lin JM, et al. Blood-brain barrier  
657 dysfunction in aging induces hyperactivation of TGFbeta signaling and chronic  
658 yet reversible neural dysfunction. *Science translational medicine*. 2019;11(521).
- 659 9. Mahmoudi S, Xu L, and Brunet A. Turning back time with emerging rejuvenation  
660 strategies. *Nat Cell Biol*. 2019;21(1):32-43.
- 661 10. Nikolich-Zugich J. Aging of the T cell compartment in mice and humans: from no  
662 naive expectations to foggy memories. *J Immunol*. 2014;193(6):2622-9.
- 663 11. Thome JJ, Yudanin N, Ohmura Y, Kubota M, Grinshpun B, Sathaliyawala T,  
664 Kato T, Lerner H, Shen Y, and Farber DL. Spatial map of human T cell  
665 compartmentalization and maintenance over decades of life. *Cell*.  
666 2014;159(4):814-28.
- 667 12. Wing K, and Sakaguchi S. Regulatory T cells exert checks and balances on self  
668 tolerance and autoimmunity. *Nat Immunol*. 2010;11(1):7-13.
- 669 13. Sakaguchi S, Yamaguchi T, Nomura T, and Ono M. Regulatory T cells and  
670 immune tolerance. *Cell*. 2008;133(5):775-87.
- 671 14. Nikolich-Zugich J. The twilight of immunity: emerging concepts in aging of the  
672 immune system. *Nat Immunol*. 2018;19(1):10-9.

- 673 15. Boraschi D, Aguado MT, Dutel C, Goronzy J, Louis J, Grubeck-Loebenstien B,  
674 Rappuoli R, and Del Giudice G. The gracefully aging immune system. *Science*  
675 *translational medicine*. 2013;5(185):185ps8.
- 676 16. Fessler J, Ficjan A, Duftner C, and Dejaco C. The impact of aging on regulatory  
677 T-cells. *Frontiers in immunology*. 2013;4(231).
- 678 17. Gregg R, Smith CM, Clark FJ, Dunnion D, Khan N, Chakraverty R, Nayak L, and  
679 Moss PA. The number of human peripheral blood CD4+ CD25high regulatory T  
680 cells increases with age. *Clin Exp Immunol*. 2005;140(3):540-6.
- 681 18. Nishioka T, Shimizu J, Iida R, Yamazaki S, and Sakaguchi S.  
682 CD4+CD25+Foxp3+ T cells and CD4+CD25-Foxp3+ T cells in aged mice. *J*  
683 *Immunol*. 2006;176(11):6586-93.
- 684 19. Vukmanovic-Stejic M, Zhang Y, Cook JE, Fletcher JM, McQuaid A, Masters JE,  
685 Rustin MH, Taams LS, Beverley PC, Macallan DC, et al. Human CD4+ CD25hi  
686 Foxp3+ regulatory T cells are derived by rapid turnover of memory populations in  
687 vivo. *J Clin Invest*. 2006;116(9):2423-33.
- 688 20. Zhao L, Sun L, Wang H, Ma H, Liu G, and Zhao Y. Changes of  
689 CD4+CD25+Foxp3+ regulatory T cells in aged Balb/c mice. *J Leukoc Biol*.  
690 2007;81(6):1386-94.
- 691 21. Kuswanto W, Burzyn D, Panduro M, Wang KK, Jang YC, Wagers AJ, Benoist C,  
692 and Mathis D. Poor Repair of Skeletal Muscle in Aging Mice Reflects a Defect in



- 693 Local, Interleukin-33-Dependent Accumulation of Regulatory T Cells. *Immunity*.  
694 2016;44(2):355-67.
- 695 22. Jagger A, Shimojima Y, Goronzy JJ, and Weyand CM. Regulatory T cells and the  
696 immune aging process: a mini-review. *Gerontology*. 2014;60(2):130-7.
- 697 23. Chougnnet CA, Tripathi P, Lages CS, Raynor J, Sholl A, Fink P, Plas DR, and  
698 Hildeman DA. A major role for Bim in regulatory T cell homeostasis. *J Immunol*.  
699 2011;186(1):156-63.
- 700 24. Raynor J, Karns R, Almanan M, Li KP, Divanovic S, Chougnnet CA, and  
701 Hildeman DA. IL-6 and ICOS Antagonize Bim and Promote Regulatory T Cell  
702 Accrual with Age. *J Immunol*. 2015;195(3):944-52.
- 703 25. Sharpless NE, and Sherr CJ. Forging a signature of in vivo senescence. *Nat Rev*  
704 *Cancer*. 2015;15(7):397-408.
- 705 26. de Magalhaes JP, Curado J, and Church GM. Meta-analysis of age-related gene  
706 expression profiles identifies common signatures of aging. *Bioinformatics*.  
707 2009;25(7):875-81.
- 708 27. Garg SK, Delaney C, Toubai T, Ghosh A, Reddy P, Banerjee R, and Yung R.  
709 Aging is associated with increased regulatory T-cell function. *Aging cell*.  
710 2014;13(3):441-8.

- 711 28. Lages CS, Suffia I, Velilla PA, Huang B, Warshaw G, Hildeman DA, Belkaid Y,  
712 and Chougnet C. Functional regulatory T cells accumulate in aged hosts and  
713 promote chronic infectious disease reactivation. *J Immunol.* 2008;181(3):1835-48.
- 714 29. Sun L, Hurez VJ, Thibodeaux SR, Kious MJ, Liu A, Lin P, Murthy K,  
715 Pandeswara S, Shin T, and Curiel TJ. Aged regulatory T cells protect from  
716 autoimmune inflammation despite reduced STAT3 activation and decreased  
717 constraint of IL-17 producing T cells. *Aging cell.* 2012;11(3):509-19.
- 718 30. Mottet C, Uhlig HH, and Powrie F. Cutting edge: cure of colitis by CD4+CD25+  
719 regulatory T cells. *J Immunol.* 2003;170(8):3939-43.
- 720 31. Chang J, Wang Y, Shao L, Laberge RM, Demaria M, Campisi J, Janakiraman K,  
721 Sharpless NE, Ding S, Feng W, et al. Clearance of senescent cells by ABT263  
722 rejuvenates aged hematopoietic stem cells in mice. *Nat Med.* 2016;22(1):78-83.
- 723 32. Duda P, Wojcicka O, Wisniewski JR, and Rakus D. Global quantitative TPA-  
724 based proteomics of mouse brain structures reveals significant alterations in  
725 expression of proteins involved in neuronal plasticity during aging. *Aging.*  
726 2018;10(7):1682-97.
- 727 33. Zhang S, Feng Y, Narayan O, and Zhao LJ. Cytoplasmic retention of HIV-1  
728 regulatory protein Vpr by protein-protein interaction with a novel human  
729 cytoplasmic protein VprBP. *Gene.* 2001;263(1-2):131-40.

- 730 34. Guo Z, Kong Q, Liu C, Zhang S, Zou L, Yan F, Whitmire JK, Xiong Y, Chen X,  
731 and Wan YY. DCAF1 controls T-cell function via p53-dependent and -  
732 independent mechanisms. *Nature communications*. 2016;7(10307).
- 733 35. Gross AM, Jaeger PA, Kreisberg JF, Licon K, Jepsen KL, Khosroheidari M,  
734 Morsey BM, Swindells S, Shen H, Ng CT, et al. Methylome-wide Analysis of  
735 Chronic HIV Infection Reveals Five-Year Increase in Biological Age and  
736 Epigenetic Targeting of HLA. *Mol Cell*. 2016;62(2):157-68.
- 737 36. Nelson JA, Krishnamurthy J, Menezes P, Liu Y, Hudgens MG, Sharpless NE, and  
738 Eron JJ, Jr. Expression of p16(INK4a) as a biomarker of T-cell aging in HIV-  
739 infected patients prior to and during antiretroviral therapy. *Aging cell*.  
740 2012;11(5):916-8.
- 741 37. Rufini A, Tucci P, Celardo I, and Melino G. Senescence and aging: the critical  
742 roles of p53. *Oncogene*. 2013;32(43):5129-43.
- 743 38. Horvath S, and Levine AJ. HIV-1 Infection Accelerates Age According to the  
744 Epigenetic Clock. *The Journal of infectious diseases*. 2015;212(10):1563-73.
- 745 39. Chiappini E, Bianconi M, Dalzini A, Petrara MR, Galli L, Giaquinto C, and De  
746 Rossi A. Accelerated aging in perinatally HIV-infected children: clinical  
747 manifestations and pathogenetic mechanisms. *Aging*. 2018;10(11):3610-25.
- 748 40. Rincon M. MAP-kinase signaling pathways in T cells. *Curr Opin Immunol*.  
749 2001;13(3):339-45.

- 750 41. Lanna A, Gomes DC, Muller-Durovic B, McDonnell T, Escors D, Gilroy DW,  
751 Lee JH, Karin M, and Akbar AN. A sestrin-dependent Erk-Jnk-p38 MAPK  
752 activation complex inhibits immunity during aging. *Nat Immunol.*  
753 2017;18(3):354-63.
- 754 42. Shapiro-Shelef M, Lin KI, Savitsky D, Liao J, and Calame K. Blimp-1 is required  
755 for maintenance of long-lived plasma cells in the bone marrow. *J Exp Med.*  
756 2005;202(11):1471-6.
- 757 43. Cagnol S, and Chambard JC. ERK and cell death: mechanisms of ERK-induced  
758 cell death--apoptosis, autophagy and senescence. *The FEBS journal.*  
759 2010;277(1):2-21.
- 760 44. Franchina DG, Dostert C, and Brenner D. Reactive Oxygen Species: Involvement  
761 in T Cell Signaling and Metabolism. *Trends in immunology.* 2018;39(6):489-502.
- 762 45. Colavitti R, and Finkel T. Reactive oxygen species as mediators of cellular  
763 senescence. *IUBMB life.* 2005;57(4-5):277-81.
- 764 46. Finkel T, and Holbrook NJ. Oxidants, oxidative stress and the biology of ageing.  
765 *Nature.* 2000;408(6809):239-47.
- 766 47. Nakagawa T, Lv L, Nakagawa M, Yu Y, Yu C, D'Alessio AC, Nakayama K, Fan  
767 HY, Chen X, and Xiong Y. CRL4(VprBP) E3 Ligase Promotes  
768 Monoubiquitylation and Chromatin Binding of TET Dioxygenases. *Mol Cell.*  
769 2015;57(2):247-60.

- 770 48. Coles BF, and Kadlubar FF. Detoxification of electrophilic compounds by  
771 glutathione S-transferase catalysis: determinants of individual response to  
772 chemical carcinogens and chemotherapeutic drugs? *BioFactors*. 2003;17(1-  
773 4):115-30.
- 774 49. Dang DT, Chen F, Kohli M, Rago C, Cummins JM, and Dang LH. Glutathione S-  
775 transferase pi1 promotes tumorigenicity in HCT116 human colon cancer cells.  
776 *Cancer Res*. 2005;65(20):9485-94.
- 777 50. Ayyadevara S, Engle MR, Singh SP, Dandapat A, Lichti CF, Benes H, Shmookler  
778 Reis RJ, Liebau E, and Zimniak P. Lifespan and stress resistance of  
779 *Caenorhabditis elegans* are increased by expression of glutathione transferases  
780 capable of metabolizing the lipid peroxidation product 4-hydroxynonenal. *Aging*  
781 *cell*. 2005;4(5):257-71.
- 782 51. Coussens LM, and Werb Z. Inflammation and cancer. *Nature*.  
783 2002;420(6917):860-7.
- 784 52. Dulken BW, Buckley MT, Navarro Negredo P, Saligrama N, Cayrol R, Leeman  
785 DS, George BM, Boutet SC, Hebestreit K, Pluvinage JV, et al. Single-cell  
786 analysis reveals T cell infiltration in old neurogenic niches. *Nature*.  
787 2019;571(7764):205-10.
- 788 53. Deeks SG, and Phillips AN. HIV infection, antiretroviral treatment, ageing, and  
789 non-AIDS related morbidity. *Bmj*. 2009;338(a3172).

- 790 54. Maj T, Wang W, Crespo J, Zhang H, Wang W, Wei S, Zhao L, Vatan L, Shao I,  
791 Szeliga W, et al. Oxidative stress controls regulatory T cell apoptosis and  
792 suppressor activity and PD-L1-blockade resistance in tumor. *Nat Immunol.*  
793 2017;18(12):1332-41.
- 794 55. Mak TW, Grusdat M, Duncan GS, Dostert C, Nonnenmacher Y, Cox M, Binsfeld  
795 C, Hao Z, Brustle A, Itsumi M, et al. Glutathione Primes T Cell Metabolism for  
796 Inflammation. *Immunity.* 2017;46(4):675-89.
- 797 56. Ray PD, Huang BW, and Tsuji Y. Reactive oxygen species (ROS) homeostasis  
798 and redox regulation in cellular signaling. *Cell Signal.* 2012;24(5):981-90.
- 799 57. Mannick JB, Del Giudice G, Lattanzi M, Valiante NM, Praestgaard J, Huang B,  
800 Lonetto MA, Maecker HT, Kovarik J, Carson S, et al. mTOR inhibition improves  
801 immune function in the elderly. *Science translational medicine.*  
802 2014;6(268):268ra179.
- 803 58. McCall CM, Miliani de Marval PL, Chastain PD, 2nd, Jackson SC, He YJ,  
804 Kotake Y, Cook JG, and Xiong Y. Human immunodeficiency virus type 1 Vpr-  
805 binding protein VprBP, a WD40 protein associated with the DDB1-CUL4 E3  
806 ubiquitin ligase, is essential for DNA replication and embryonic development.  
807 *Mol Cell Biol.* 2008;28(18):5621-33.
- 808 59. Lee PP, Fitzpatrick DR, Beard C, Jessup HK, Lehar S, Makar KW, Perez-  
809 Melgosa M, Sweetser MT, Schlissel MS, Nguyen S, et al. A critical role for

- 810 Dnmt1 and DNA methylation in T cell development, function, and survival.  
811 *Immunity*. 2001;15(5):763-74.
- 812 60. Debacq-Chainiaux F, Erusalimsky JD, Campisi J, and Toussaint O. Protocols to  
813 detect senescence-associated beta-galactosidase (SA-beta-gal) activity, a  
814 biomarker of senescent cells in culture and in vivo. *Nature protocols*.  
815 2009;4(12):1798-806.
- 816 61. Jackson SH, Devadas S, Kwon J, Pinto LA, and Williams MS. T cells express a  
817 phagocyte-type NADPH oxidase that is activated after T cell receptor stimulation.  
818 *Nat Immunol*. 2004;5(8):818-27.
- 819 62. Patro R, Duggal G, Love MI, Irizarry RA, and Kingsford C. Salmon provides fast  
820 and bias-aware quantification of transcript expression. *Nat Methods*.  
821 2017;14(4):417-9.
- 822 63. Sonesson C, Love MI, and Robinson MD. Differential analyses for RNA-seq:  
823 transcript-level estimates improve gene-level inferences. *F1000Research*.  
824 2015;4(1521).
- 825 64. Love MI, Huber W, and Anders S. Moderated estimation of fold change and  
826 dispersion for RNA-seq data with DESeq2. *Genome biology*. 2014;15(12):550.
- 827 65. Subramanian A, Tamayo P, Mootha VK, Mukherjee S, Ebert BL, Gillette MA,  
828 Paulovich A, Pomeroy SL, Golub TR, Lander ES, et al. Gene set enrichment  
829 analysis: a knowledge-based approach for interpreting genome-wide expression  
830 profiles. *Proc Natl Acad Sci U S A*. 2005;102(43):15545-50.

831 66. Liberzon A, Subramanian A, Pinchback R, Thorvaldsdottir H, Tamayo P, and  
832 Mesirov JP. Molecular signatures database (MSigDB) 3.0. *Bioinformatics*.  
833 2011;27(12):1739-40.  
834



835 **Figure Legends**

836 **Fig. 1. Preferential Treg cell ageing in young and aged mice.**

837 **(A)** Proliferation of CD4<sup>+</sup>Foxp3<sup>+</sup> (Treg) and CD4<sup>+</sup>Foxp3<sup>-</sup> (Tconv) cells from young and  
838 aged (more than 18-month old) mice 3 days after activation when cultured in same well,  
839 analyzed by CFSE dilution and flow-cytometry (n=7 mice of three experiments;  
840 representative results are shown; means ± s.d., \*\*\*\**p*<0.0001, by one-way ANOVA post  
841 Turkey's multiple comparisons test).

842 **(B)** SA-β-gal activity of CD4<sup>+</sup>CD25<sup>+</sup> Treg and CD4<sup>+</sup>CD25<sup>-</sup> Tconv cells in the  
843 splenocytes from young and aged mice, assessed by flow-cytometry with the fluorescent  
844 β-gal substrate C<sub>12</sub>FDG (grey area, no C<sub>12</sub>FDG; n= 6 mice of three experiments;  
845 representative flow-cytometry results are shown; means ± s.d., \*\*\*\**p*<0.0001, by one-  
846 way ANOVA post Turkey's multiple comparisons test).

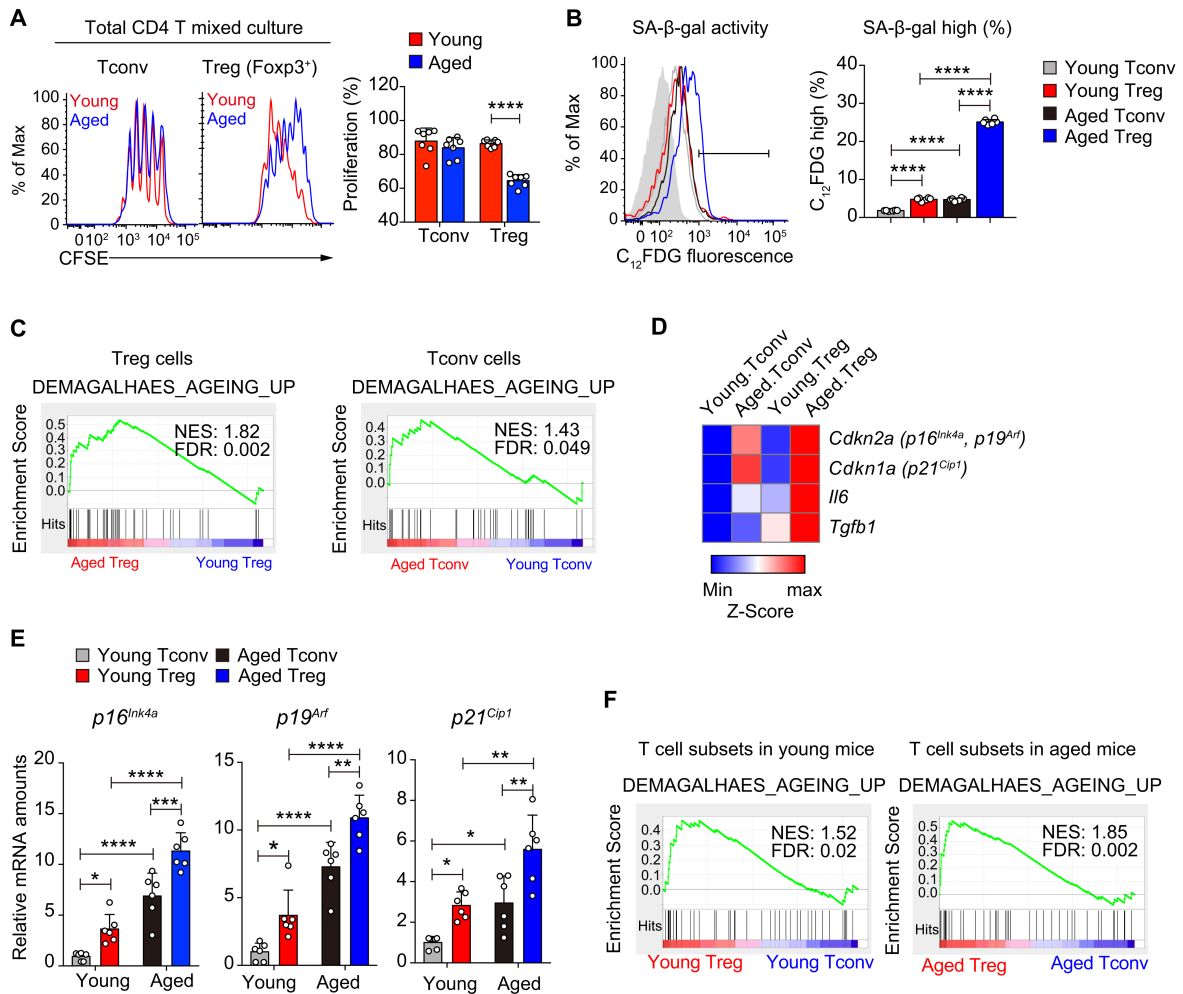
847 **(C)** Elevated ageing-program in aged Treg cells (upper panel) and aged Tconv cells  
848 (lower panel) revealed by GSEA analysis of RNA-seq datasets.

849 **(D-E)** Preferential upregulation of senescence signature genes in aged Treg cells,  
850 revealed by heatmap analysis of RNA-seq datasets **(D)** and by qRT-PCR analysis of  
851 indicated genes (n=6 mice of three experiments; means ± s.d., \**p*<0.05, \*\**p*<0.01,  
852 \*\*\**p*<0.001, \*\*\*\**p*<0.0001, by one-way ANOVA post Turkey's multiple comparisons  
853 test) **(E)**.

854 **(F)** Preferential upregulation of ageing-program in Treg cells in both young (upper panel)  
855 and aged (lower panel) mice, revealed by GSEA analysis of RNA-seq datasets.

856

Fig. 1



857 **Fig. 2. Deterioration of Treg cell function in aged mice.**

858 **(A-B)** Comparison of the suppressive activity of young and aged Treg cells by *in vitro*  
859 suppression assays **(A)**. The composition of Foxp3<sup>+</sup> Treg cells was also assessed by flow-  
860 cytometry **(B)**. (n=3 mice of three experiments; representative results are shown; means ±  
861 s.d., \*\**p*<0.01, \*\*\*\**p*<0.0001, by two-way ANOVA post Sidak's multiple comparisons  
862 test)

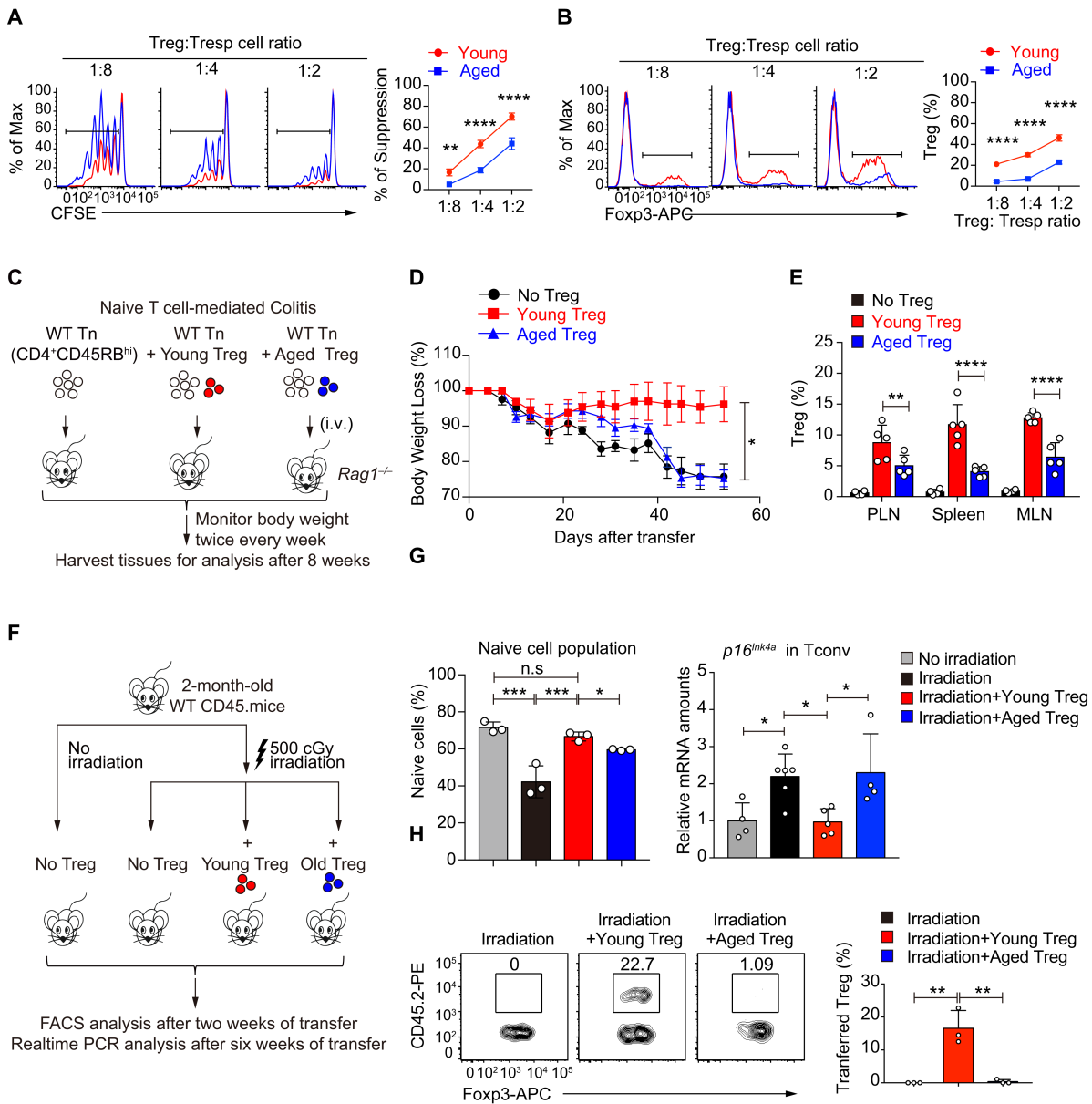
863 **(C-D)** Schematic diagram of T cell-induced colitis **(C)**. *Rag1*<sup>-/-</sup> recipients received WT  
864 naïve CD4<sup>+</sup>CD45RB<sup>hi</sup> T cells (Tn) alone or in combination with young or aged  
865 CD4<sup>+</sup>CD25<sup>+</sup> Treg cells. After transfer, the body weight loss was monitored to examine  
866 the suppressive ability of young and old Treg cells **(D)**. (n=10 mice per group of two  
867 experiments; means ± s.e.m., \**p*<0.05 for young Treg vs no Treg, *p*= 0.3682 for aged  
868 Treg vs no Treg, \**p*< 0.05 for young Treg vs aged Treg, by two-way-ANOVA followed  
869 by Holm-Sidak test)

870 **(E)** The percentages of Treg cells recovered in periphery lymph nodes (PLN), spleens  
871 and mesenteric lymph nodes (MLN) in the recipient mice at the end of the experiments  
872 (n=5 mice of two experiments; means ± s.d., \*\**p*<0.01, \*\**p*<0.01, by two-way ANOVA  
873 post Sidak's multiple comparisons test).

874 **(F-H)** Schematic diagram of whole-body irradiation induced senescence **(F)**. WT CD45.1  
875 mice were sub-lethally irradiated and transferred with or without young or aged  
876 CD4<sup>+</sup>CD25<sup>+</sup> Treg cells. The naïve T cell population (CD62L<sup>hi</sup>CD44<sup>low</sup>CD45.1<sup>+</sup>) **(G, left)**  
877 and *p16*<sup>Ink4a</sup> mRNA expression **(G, right)** of host Tconv cells in the indicated group of  
878 mice were analyzed. The percentage of transferred Treg cells (CD45.2<sup>+</sup>) among host Treg  
879 cells in the recipient mice (CD45.1<sup>+</sup>) was analyzed by flow-cytometry **(H)**. (n=3-5 mice  
880 of three experiments; means ± s.d., n.s., not significant, \**p*<0.05, \*\**p*<0.01\*\*\**p*<0.001,  
881 by one-way ANOVA post Turkey's multiple comparisons test).

882

Fig. 2



883 **Fig. 3. DCAF1 deletion led to T cell ageing in young mice.**

884 **(A)** Protein expression of DCAF1 in Treg cells isolated from young and aged mice,  
885 assessed by immunoblotting. Left, representative of three independent experiments;  
886 Right, statistical summary, means  $\pm$  s.d., \* $p$ <0.05, by Mann-Whitney's U test.

887 **(B)** SA- $\beta$ -gal activity in CD4<sup>+</sup>CD25<sup>+</sup> Treg and CD4<sup>+</sup>CD25<sup>-</sup> Tconv cells in the  
888 splenocytes from mice of indicated genotypes, analyzed by flow-cytometry with the  
889 fluorescent  $\beta$ -gal substrate C<sub>12</sub>FDG (grey area, no C<sub>12</sub>FDG; n=6 mice of three  
890 experiments; representative results are shown; means  $\pm$  s.d., \*\*\*\* $p$ <0.0001, by one-way  
891 ANOVA post Turkey's multiple comparison)

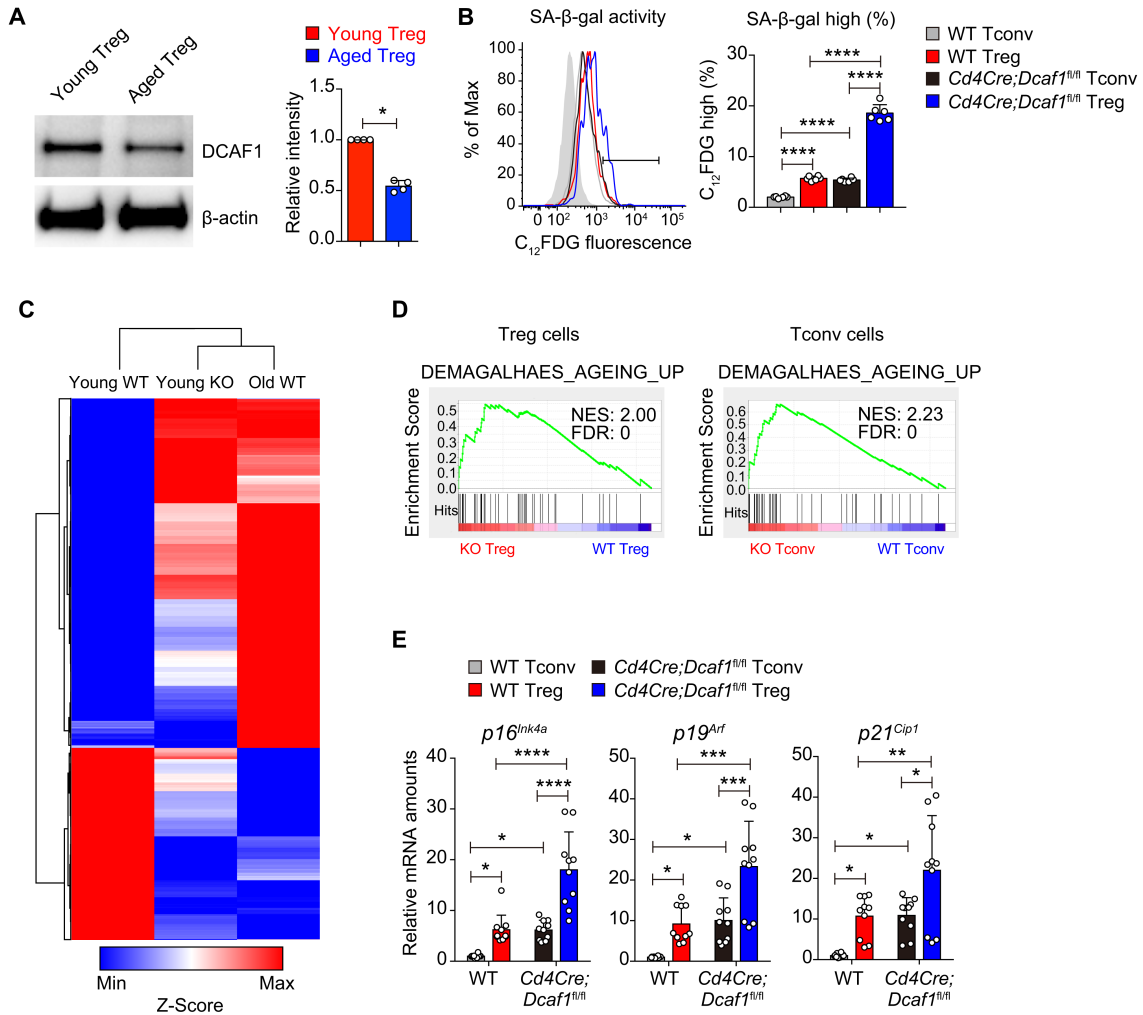
892 **(C)** Heatmap analysis of RNA-seq datasets to compare top regulated genes in young  
893 wild-type (WT), young Dcaf1-deficient (KO) and aged WT Treg cells. The depicted  
894 distance was calculated based on Pearson's correlation.

895 **(D)** Upregulation of ageing-program in Dcaf1-deficient (KO) Treg (left) and Tconv cells  
896 (right) cells, revealed by GSEA analysis of RNA-seq datasets.

897 **(E)** Comparison of ageing signature gene expression in indicated T cells by qRT-PCR  
898 analysis of indicated genes (n=10 mice of four experiments; means  $\pm$  s.d., \* $p$ <0.05,  
899 \*\* $p$ <0.01, \*\*\* $p$ <0.001, \*\*\*\* $p$ <0.0001, by one-way ANOVA post Turkey's multiple  
900 comparisons test).

901

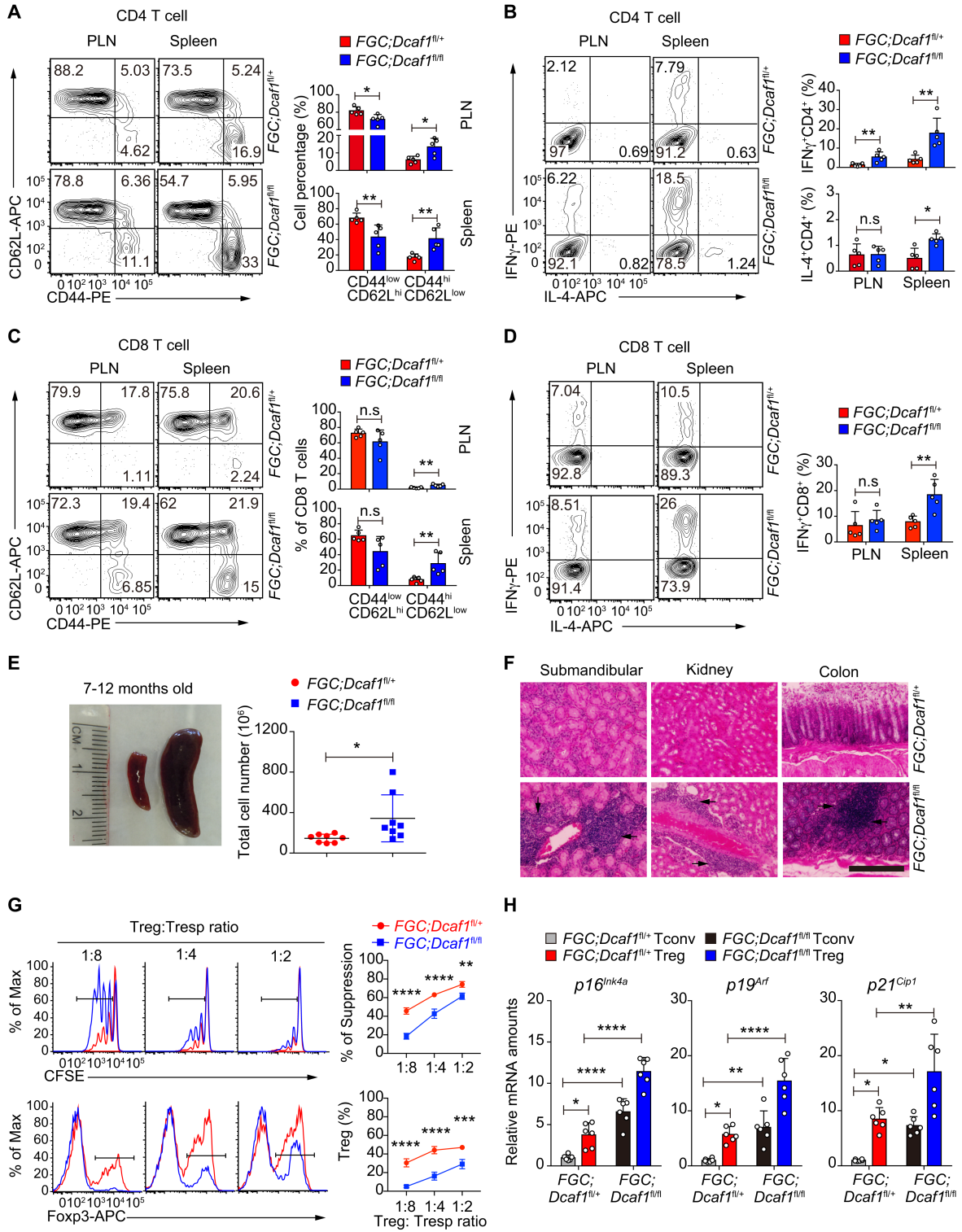
Fig. 3



902 **Fig. 4. DCAF1 is required to prevent Treg cell ageing and inflamm-ageing.**  
903 **(A-B)** Distribution of naïve and effector/memory CD4 T cells **(A)** and IFN $\gamma$  and IL-4  
904 production of CD4 T cells **(B)** in peripheral lymph nodes (PLN) and spleens of 2-month-  
905 old mice of indicated genotypes, assessed by flow-cytometry (n=5 mice of five  
906 experiments; representative results are shown; means  $\pm$  s.d., \* $p$ <0.05, \*\* $p$ <0.01, by  
907 Mann-Whitney's U test).  
908 **(C-D)** Distribution of naïve and effector/memory CD8 T cells **(C)** and IFN $\gamma$  and IL-4  
909 production of CD8 T cells **(D)** in peripheral lymph nodes (PLN) and spleens of 2-month-  
910 old mice of indicated genotypes, assessed by flow-cytometry (n=5 mice of five  
911 experiments; representative results are shown; means  $\pm$  s.d., \*\* $p$ <0.01, by Mann-  
912 Whitney's U test).  
913 **(E)** Splenomegaly (left) and increased splenocyte counts (right) in 7- to 12-month-old  
914 *FGC;Dcaf1<sup>fl/fl</sup>* mice (n=8 mice of eight experiments; representative results are shown,  
915 means  $\pm$  s.d., \* $p$ <0.05, per two-sided *t*-test).  
916 **(F)** Histology to compare lymphocytic infiltration in the submandibular gland, kidney  
917 and colon in 7-12-month-old littermates of indicated genotypes (Scale bar, 100  $\mu$ m;  
918 arrows indicate lymphocyte infiltration foci; results are representative of five mice).  
919 **(G)** Comparison of the suppressive activity of Treg cells of indicated genotype by *in vitro*  
920 suppression assays (upper panels). The composition of Foxp3<sup>+</sup> Treg cells was also  
921 assessed by flow-cytometry (lower panels) (n=3 mice of three experiments;  
922 representative results are shown; means  $\pm$  s.d., \*\* $p$ <0.01, \*\*\* $p$ <0.001, \*\*\*\* $p$ <0.0001, by  
923 two-way ANOVA post Sidak's multiple comparisons test)  
924 **(H)** Comparison of ageing signature gene expression in Treg and Tconv cells from mice  
925 of indicated genotypes, assessed by qRT-PCR analysis of indicated genes (n=6 mice of  
926 six experiments; means  $\pm$  s.d., \* $p$ <0.05, \*\* $p$ <0.01, \*\*\*\* $p$ <0.0001, by one-way ANOVA  
927 post Turkey's multiple comparisons test)

928

Fig. 4





929 **Fig. 5. Dcaf1-deficient Treg cells co-op inflammation to promote the ageing of Tconv**  
930 **cells.**

931 **(A)** Schematic diagram for the generation of mixed bone marrow chimeric mice to  
932 contain both *FGC;Dcaf1<sup>fl/+</sup>* (CD45.1.2) and *FGC;Dcaf1<sup>fl/fl</sup>* (CD45.2) T cells.

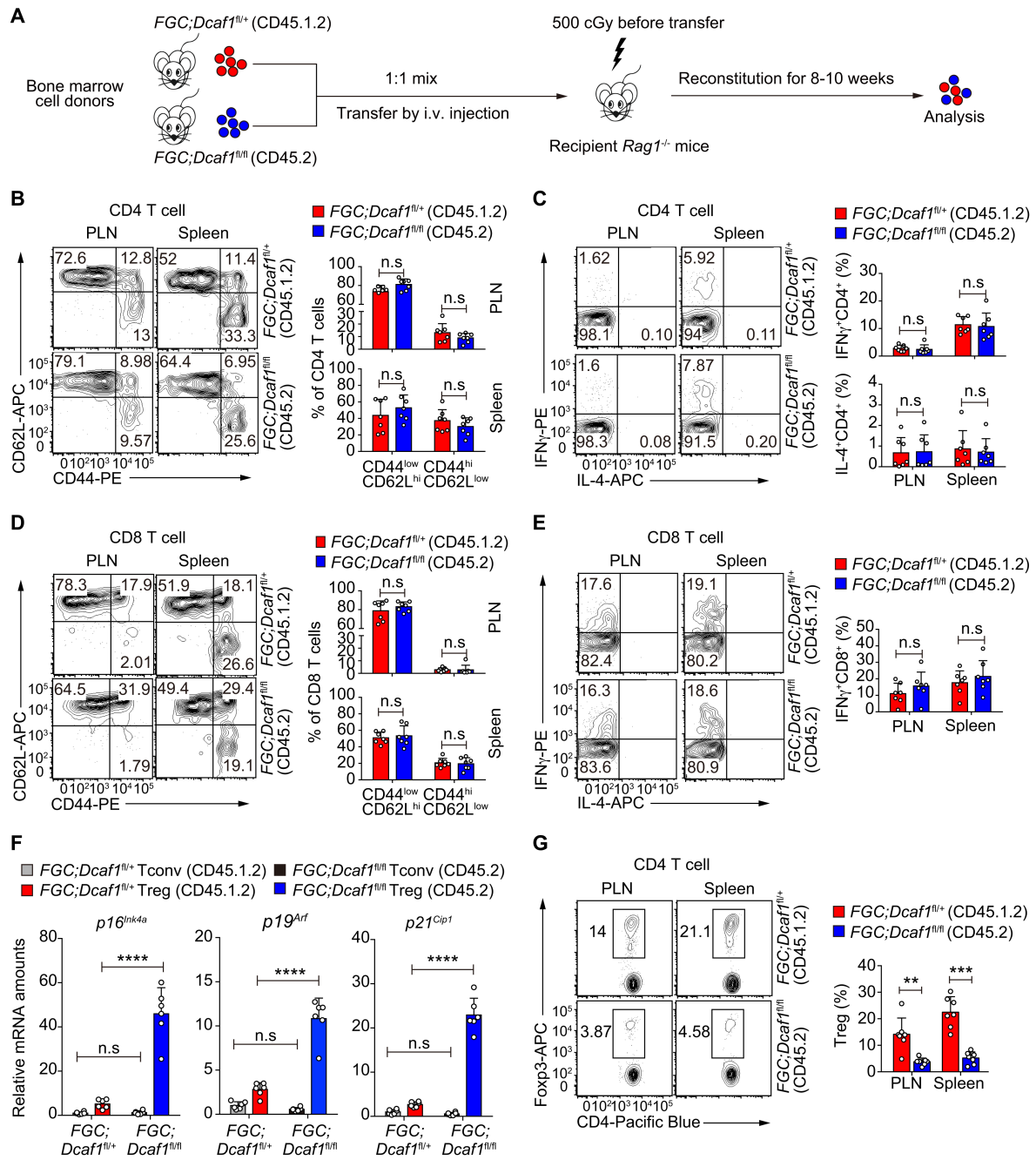
933 **(B-E)** Flow-cytometry of CD44/CD62L expression **(B)** and cytokine production **(C)** by  
934 CD4 T cells of indicated genotypes, of CD44/CD62L expression **(D)** and cytokine  
935 production **(E)** by CD8 T cells of indicated genotypes, in peripheral lymph nodes (PLN)  
936 and spleens of the mixed bone marrow chimeric mice generated as described in **A** (n=7  
937 mice of seven experiments; representative results are shown; means  $\pm$  s.d., n.s., not  
938 significant, by Mann-Whitney's U test).

939 **(F)** Comparison of ageing signature gene expression in Treg and Tconv cells of indicated  
940 genotypes in mixed bone marrow chimera mice generated as described in **A** (n=6 mice of  
941 three experiments; means  $\pm$  s.d., n.s., not significant,  $**p < 0.01$ , by Mann-Whitney's U  
942 test).

943 **(G)** Flow-cytometry of Treg cells of indicated genotypes in peripheral lymph nodes  
944 (PLN) and spleens of the mixed bone marrow chimeric mice generated as described in **A**  
945 (n=7 mice of seven experiments; representative results are shown; means  $\pm$  s.d., n.s., not  
946 significant,  $****p < 0.0001$ , by one-way ANOVA post Turkey's multiple comparisons  
947 test).

948

Fig. 5



949 **Fig. 6. DCAF1 is required to prevent human T cell ageing.**

950 **(A)** The protein expression of DCAF1 and  $\beta$ -actin in human 293T cells transduced with  
951 lentivirus expressing two shRNA targeting *Dcaf1* and scrambled control for 4 days. The  
952 results are representative of three independent experiments.

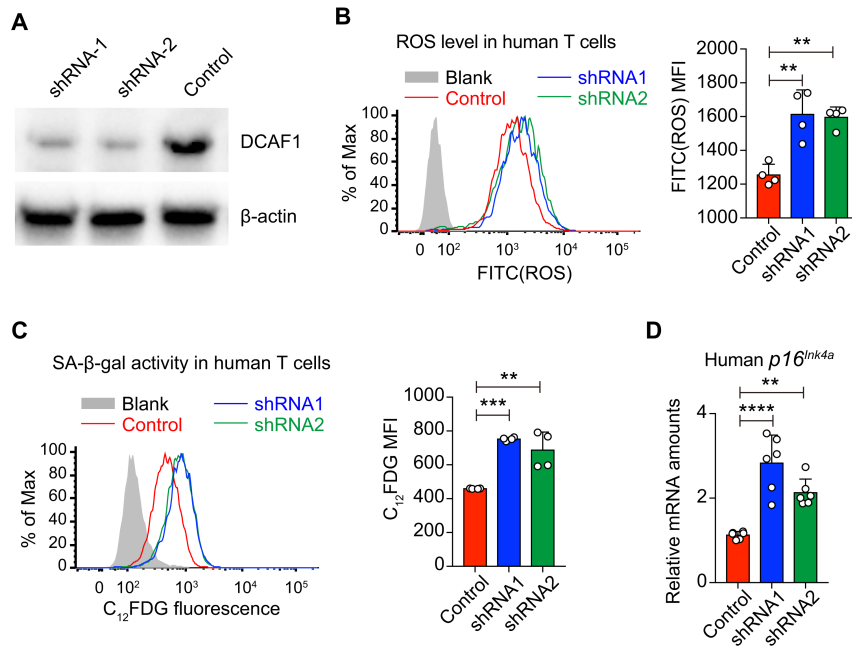
953 **(B)** Flow-cytometry of ROS level in human T cells transduced with lentivirus expressing  
954 two shRNA targeting *Dcaf1* and scrambled control for 4 days, analyzed by DCFDA (grey  
955 area, no DCFDA; n=4; representative results of two independent experiments are shown;  
956 means  $\pm$  s.d., \*\* $p$ <0.01, by one-way ANOVA post Turkey's multiple comparisons test).

957 **(C)** SA- $\beta$ -gal activity in human T cells transduced with lentivirus expressing two shRNA  
958 targeting *Dcaf1* and scrambled control for 6 days, assessed by flow-cytometry with the  
959 fluorescent  $\beta$ -gal substrate C<sub>12</sub>FDG (grey area, no C<sub>12</sub>FDG; n= 4; representative flow-  
960 cytometry results are shown; means  $\pm$  s.d., \*\* $p$ <0.01, \*\*\* $p$ <0.001, by one-way ANOVA  
961 post Turkey's multiple comparisons test).

962 **(D)** qRT-PCR analysis to determine mRNA expression of *p16<sup>Ink4a</sup>* in human T cells  
963 transduced with two shRNA targeting *Dcaf1* and scrambled control for 6 days (n=6 from  
964 two independent experiments; means  $\pm$  s.d., \*\* $p$ <0.01, \*\*\*\* $p$ <0.0001, by one-way  
965 ANOVA post Turkey's multiple comparisons test).

966

Fig. 6



967 **Fig. 7. DCAF1 is required to suppress ROS in Treg cells.**

968 **(A)** Pathways commonly enriched in aged and *Dcaf1*-deficient (*CD4Cre;Dcaf1<sup>fl/fl</sup>*) Treg  
969 cells based on GSEA analysis of RNA-seq datasets (FDR<0.05).

970 **(B)** Enrichment of ROS pathway in aged vs. young WT Treg cells (upper panel) and  
971 *Dcaf1*-deficient (KO) vs. wild-type (WT) Treg cells (lower panel) by GSEA of RNA-seq  
972 datasets.

973 **(C-D)** Flow-cytometry of ROS level in indicated T cell populations from young wild-  
974 type mice (WT) and aged wild-type mice **(C)** and young *Dcaf1*-deficient mice **(D)**,  
975 analyzed by DCFDA (grey area, no DCFDA; n=3 mice of three experiments;  
976 representative results are shown; means  $\pm$  s.d., \*\* $p$ <0.01, \*\*\* $p$ <0.001, \*\*\*\* $p$ <0.0001, by  
977 two-way ANOVA post Sidak's multiple comparisons test).

978 **(E)** Flow-cytometry of ROS level in activated wild-type (WT) and *ERCre;Dcaf1<sup>fl/fl</sup>* CD4  
979 T cells treated with 4-hydroxy-tamoxifen for indicated days, analyzed by DCFDA (n=3  
980 mice of three experiments; representative results are shown; means  $\pm$  s.d., \*\* $p$ <0.01, by  
981 two-way ANOVA post Sidak's multiple comparisons test).

982 **(F-G)** Interaction of GSTP1 and DCAF1 by co-immunoprecipitation in 293T cells **(F)**  
983 and by endogenous immunoprecipitation using anti-DCAF1 antibody in mouse T cells  
984 **(G)**. The results were representative of three independent experiments.

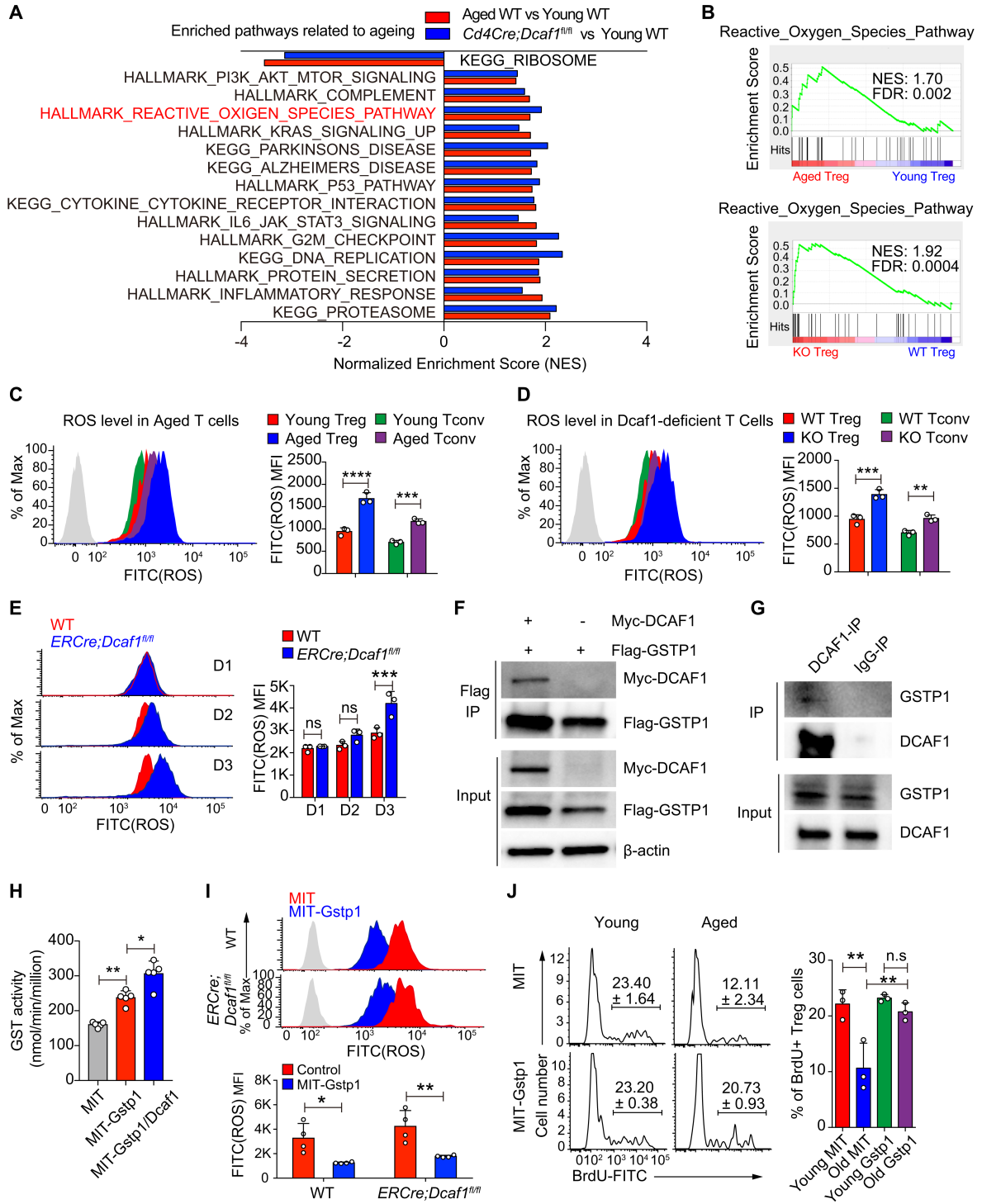
985 **(H)** The glutathione S-transferases (GST) activity in 293T cells after overexpression of  
986 GSTP1 and DCAF1 for 4 days; n=5; means  $\pm$  s.d., \* $p$ <0.05, \*\* $p$ <0.01, by Mann-  
987 Whitney's U test.

988 **(I)** Flow-cytometry of ROS level in activated wild-type (WT) and *ERCre;Dcaf1<sup>fl/fl</sup>* CD4  
989 T cells transduced with MIT (MSCV-IRES-Thy1.1) or MIT-*Gstp1* virus in the presence  
990 of 4-hydroxy-tamoxifen, analyzed by DCFDA (grey area, no DCFDA; n=3-4  
991 experiments; means  $\pm$  s.d., \* $p$ <0.01, \*\* $p$ <0.05, by two-way ANOVA post Sidak's  
992 multiple comparisons test).

993 **(J)** Proliferation assayed by BrdU incorporation in young and aged Treg cells transduced  
994 with MIT or MIT-*Gstp1* virus. (n=3 experiments; means  $\pm$  s.d., n.s. not significant,  
995 \*\* $p$ <0.01, by one-way ANOVA post Turkey's multiple comparison)

996

Fig. 7



997 **Fig. 8. ROS is important for Treg cell ageing and functional deterioration.**

998 **(A-B)** Flow-cytometry of ROS levels in aged Treg cells **(A)** and Dcaf1-deficient  
999 (*CD4Cre;Dcaf1<sup>fl/fl</sup>*) Treg cells **(B)** in the absence (-) or presence (+) of NAC (20 mM) or  
1000 GSH (10 mM) (Blank, no DCFDA; n=3 mice of three experiments; representative results  
1001 are shown; means  $\pm$  s.d., \*\*\*\* $p$ <0.0001, by one-way ANOVA post Turkey's multiple  
1002 comparison).

1003 **(C)** Proliferation assayed by BrdU incorporation in aged Treg cells in the absence (-) or  
1004 presence (+) of NAC (20 mM) or GSH (10 mM) (n=4 mice of four experiments;  
1005 representative results are shown; means  $\pm$  s.d., \*\*\* $p$ <0.001, \*\*\*\* $p$ <0.0001, by one-way  
1006 ANOVA post Turkey's multiple comparison).

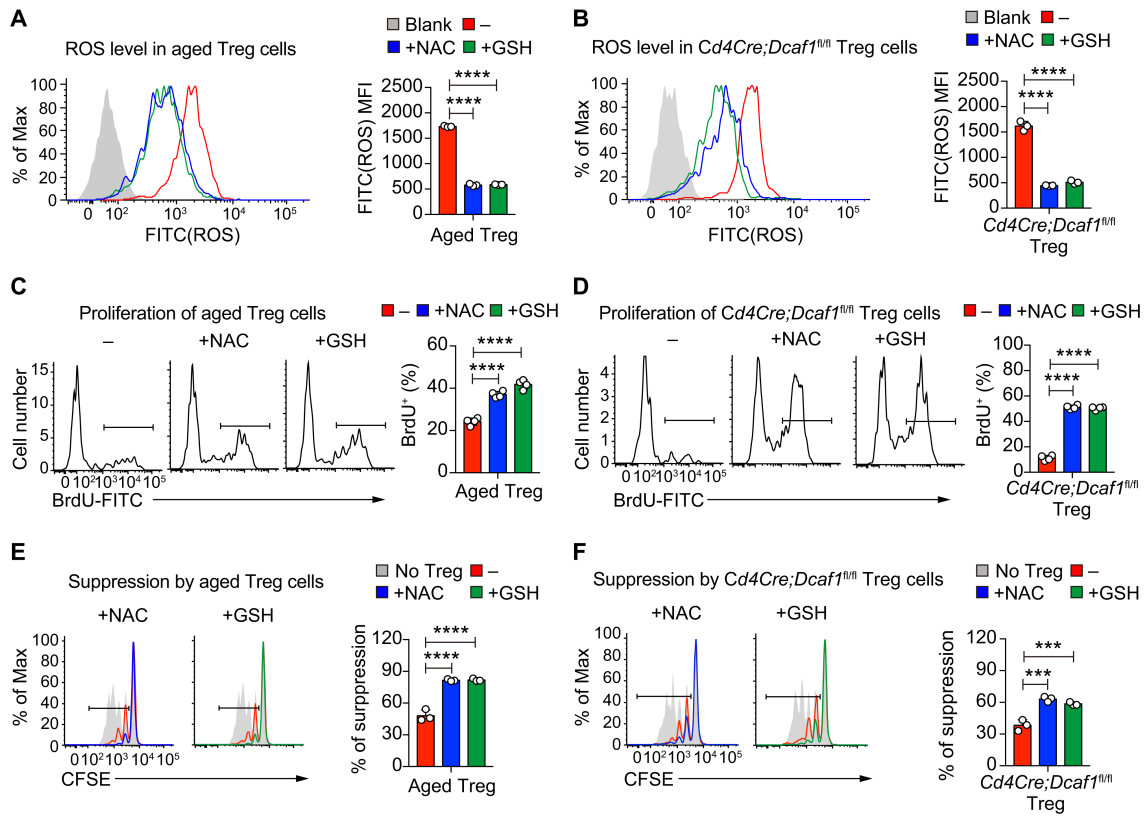
1007 **(D)** Proliferation assayed by BrdU incorporation in Dcaf1-deficient (*CD4Cre;Dcaf1<sup>fl/fl</sup>*)  
1008 Treg cells in the absence (-) or presence (+) of NAC (20 mM) or GSH (10 mM) (n=4  
1009 mice of four experiments; representative results are shown; means  $\pm$  s.d., \*\*\*\* $p$ <0.0001,  
1010 by one-way ANOVA post Turkey's multiple comparison).

1011 **(E)** The suppressive activity of aged Treg cells without (-) or with (+) pretreatment of  
1012 NAC (20 mM) or GSH (10 mM), assessed by *in vitro* suppression assay (n=3 mice of  
1013 three experiments; representative results are shown; means  $\pm$  s.d., \*\*\*\* $p$ <0.0001, by one-  
1014 way ANOVA post Turkey's multiple comparison)

1015 **(F)** The suppressive activity of Dcaf1-deficient (*CD4Cre;Dcaf1<sup>fl/fl</sup>*) Treg cells without (-)  
1016 or with (+) pretreatment of NAC (20 mM) or GSH (10 mM), assessed by *in vitro*  
1017 suppression assays (n=3 mice of three experiments; representative results are shown;  
1018 means  $\pm$  s.d., \*\*\* $p$ <0.001, by one-way ANOVA post Turkey's multiple comparison).

1019

Fig. 8





1020 **Supplementary Figure legends**

1021 **Fig. S1. T cell homeostasis and ageing in aged mice**

1022 **(A-B)** Distribution of naïve and effector/memory CD4 **(A)** and CD8 **(B)** T cells in  
1023 peripheral lymph nodes (PLN) and spleens of young and aged mice, assessed by flow-  
1024 cytometry (n=6 mice of six experiments; representative results are shown; means  $\pm$  s.d.,  
1025  $**p<0.01$ ,  $***p<0.001$ , by Mann-Whitney's U test).

1026 **(C-D)** IFN $\gamma$  and IL-4 production by CD4 **(C)** and CD8 **(D)** T cells in peripheral lymph  
1027 nodes (PLN) and spleens of young and aged mice, assessed by flow-cytometry (n=6 mice  
1028 of six experiments; representative results are shown; means  $\pm$  s.d.,  $**p<0.01$ , by Mann-  
1029 Whitney's U test).

1030 **(E)** The proliferation of young and aged Treg cells co-cultured with Tconv cells analyzed  
1031 by BrdU incorporation and flow-cytometry (n=3 mice of three experiments; means  $\pm$  s.d.,  
1032  $*p<0.05$ ,  $***p<0.001$ ,  $****p<0.0001$ , by two-way ANOVA post Sidak's multiple  
1033 comparisons test).

1034 **(F)** Purity of isolated CD4<sup>+</sup>CD25<sup>+</sup> Tregs from WT and aged mice. Flow-cytometry of  
1035 CD4<sup>+</sup>CD25<sup>+</sup>Foxp3<sup>+</sup> Tregs shows that more than 97% of isolated Tregs are Foxp3<sup>+</sup> cells.

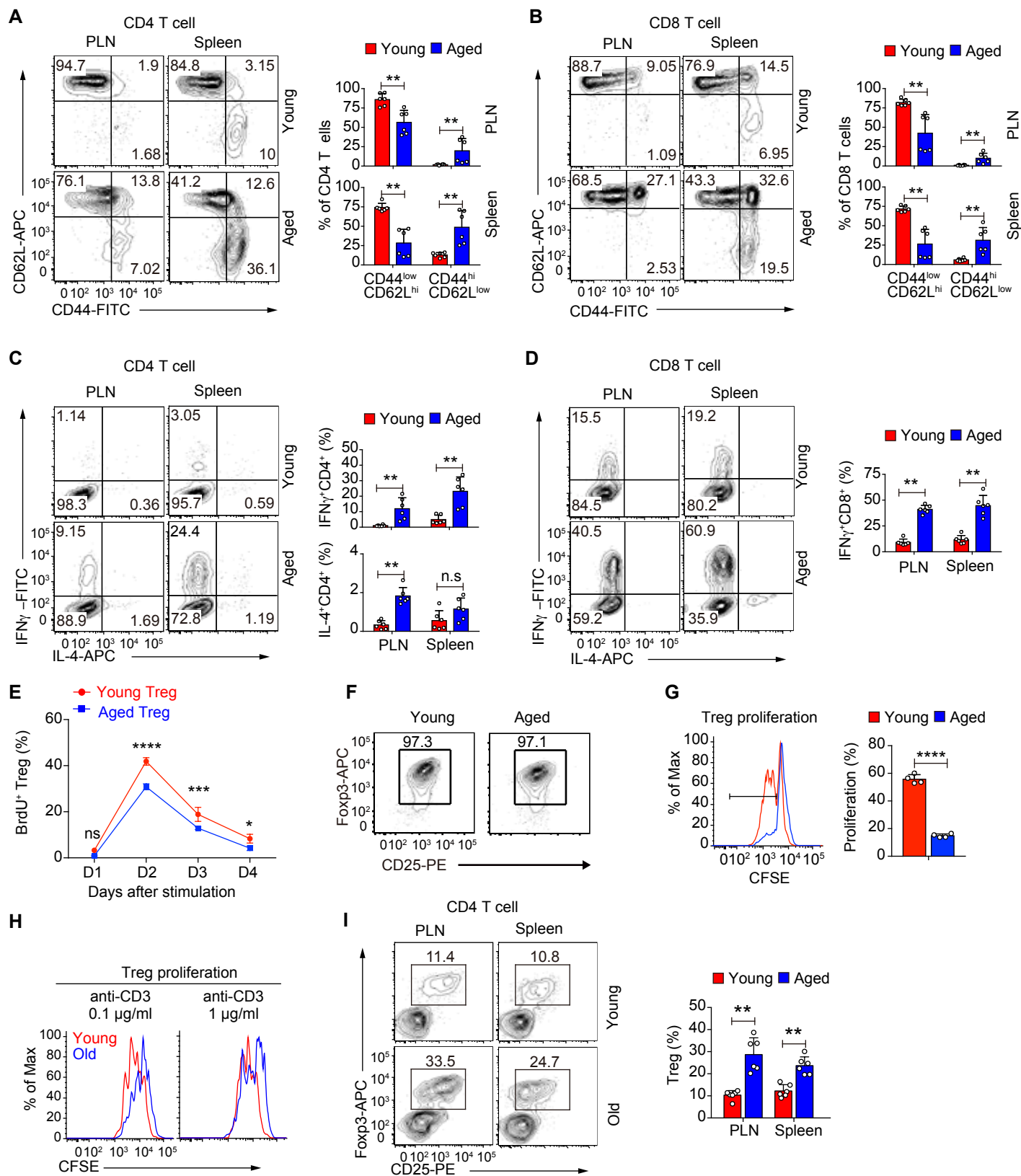
1036 **(G)** The proliferation of young and aged Treg cells stimulated with anti-CD3 and anti-  
1037 CD28 antibodies coated in 24-well plate in the presence of IL-2, without CD4 Tconv cell  
1038 coculture (n=4 mice; representative results are shown; means  $\pm$  s.d.,  $****p<0.0001$ , by  
1039 Mann-Whitney's U test).

1040 **(H)** The proliferation of young and aged Treg cells activated by different dose of anti-  
1041 CD3 antibodies analyzed by CFSE dilution and flow-cytometry. The FACS plots are  
1042 representative of three independent experiments.

1043 **(I)** The population of CD4<sup>+</sup>CD25<sup>+</sup>Foxp3<sup>+</sup> Treg cells in peripheral lymph nodes (PLN)  
1044 and spleens of young and aged mice, assessed by flow-cytometry (n=6 mice of six  
1045 experiments; representative results are shown; means  $\pm$  s.d.,  $**p<0.001$ , by Mann-  
1046 Whitney's U test).

1047

Fig. S1



1048 **Fig. S2. Treg signature gene expression in aged Treg cells and Treg cell population**  
1049 **in naive T cell induced colitis model**

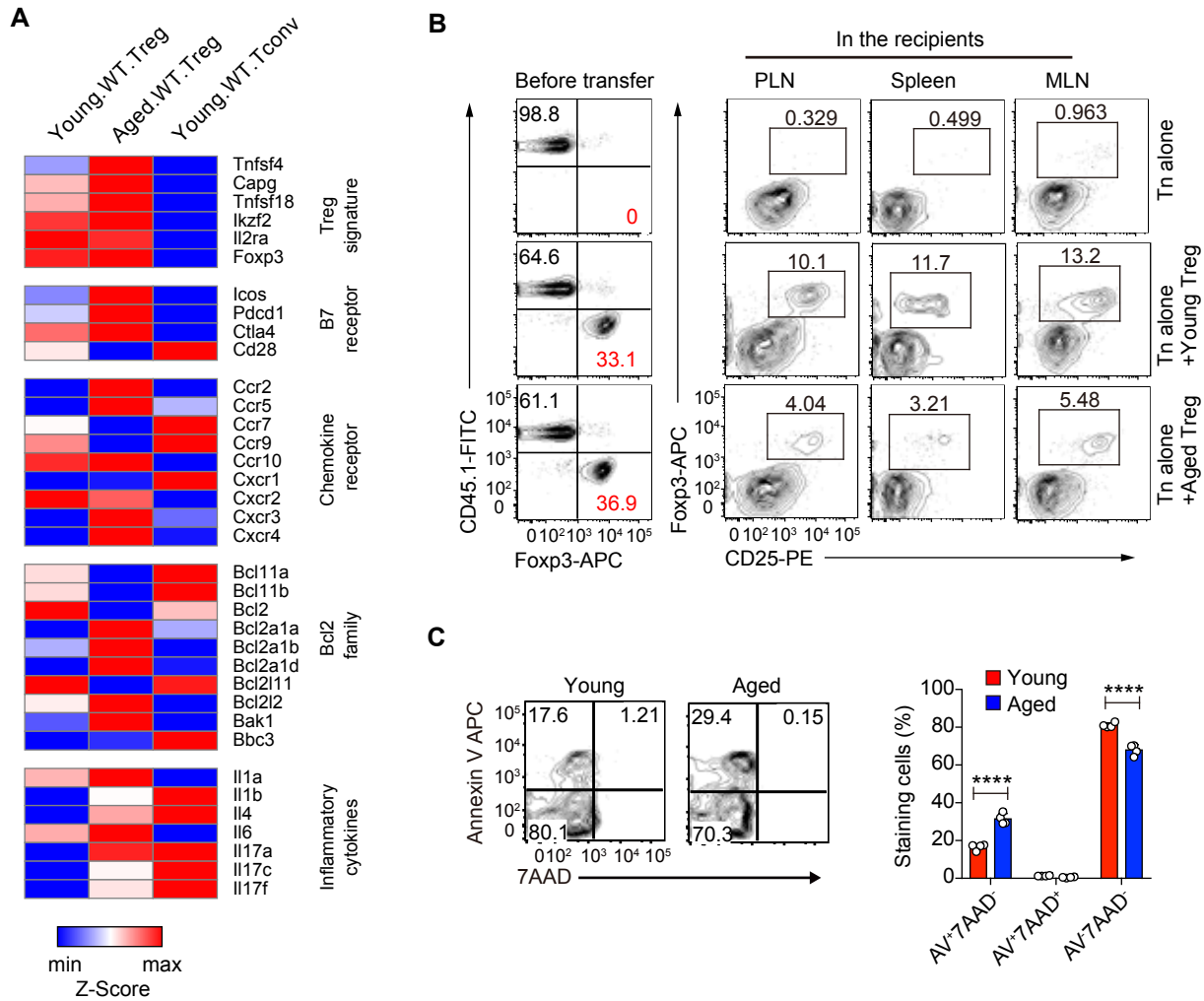
1050 **(A)** Comparison of the expression of Treg signature, B7 receptor family, chemokine  
1051 receptor family, Bcl2 family and inflammatory cytokine family genes in young and aged  
1052 Treg cells as well as young Tconv cells by heatmap analysis of RNA-seq datasets.

1053 **(B)** Flow-cytometry of T cell population distribution before and 8 weeks after the transfer  
1054 of indicated cell mixtures into *Rag1*<sup>-/-</sup> recipient mice (Results are representative of five  
1055 experiments).

1056 **(C)** Apoptosis of young and aged Tregs in spleen was analyzed by flow-cytometry using  
1057 Annexin V and 7AAD staining. Left, representative sample; right, composite data of 4  
1058 mice; n=4 mice; means ± s.d., \*\*\*\**p*<0.0001, by two-way ANOVA post Sidak's multiple  
1059 comparisons test.

1060

Fig. S2



1061 **Fig. S3. DCAF1 controls Treg cell function and immune homeostasis**

1062 **(A)** The protein amount of DCAF1 in the cortex and cerebellum of young (1-month) and  
1063 aged (12-month) mice, analyzed by mass spectrometry according to a previous  
1064 publication.

1065 **(B)** The protein expression of DCAF1 in Treg and Tconv cells from mice of indicated  
1066 genotypes, assessed by immune-blotting. The results are representative of three  
1067 experiments.

1068 **(C)** Flow-cytometry of Treg cells in mice of indicated genotypes (n=5 mice of five  
1069 experiments; representative results are shown; means  $\pm$  s.d., n.s., not significant, by  
1070 Mann-Whitney's U test).

1071 **(D)** Comparison of the expression of Treg signature, B7 receptor family, chemokine  
1072 receptor family, Bcl2 family and inflammatory cytokine family genes in young WT and  
1073 young Dcaf1-deficient Treg cells as well as young WT Tconv cells by heatmap analysis  
1074 of RNA-seq datasets.

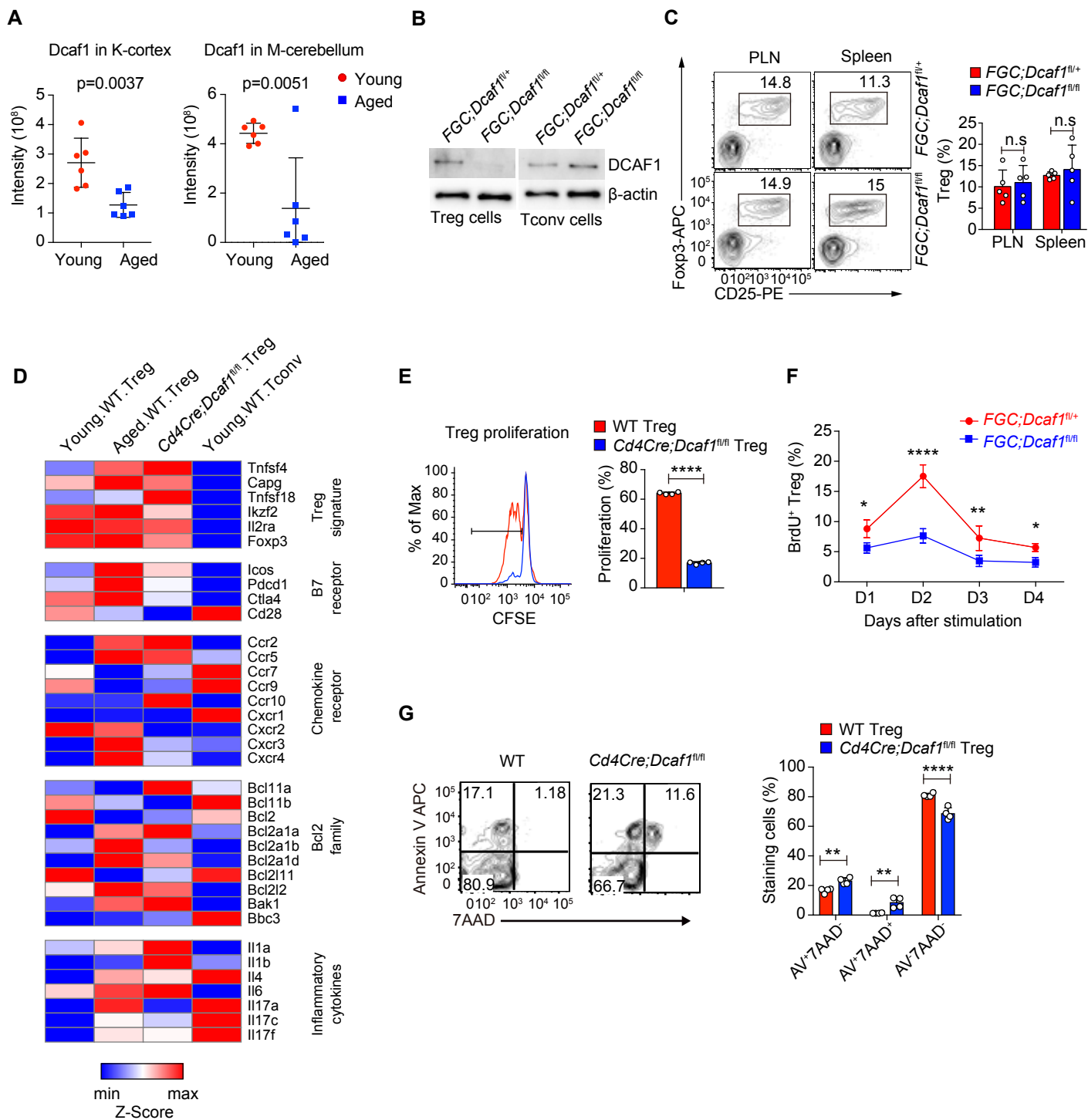
1075 **(E)** The proliferation of WT and Dcaf1-deficient Treg cells stimulated with anti-CD3 and  
1076 anti-CD28 antibodies coated in 24-well plate in the presence of IL-2, without CD4 Tconv  
1077 cell coculture. Left, representative FACS plot; right, composite data of 4 mice; n=4 mice;  
1078 representative results are shown; means  $\pm$  s.d., \*\*\*\* $p$ <0.0001, by Mann-Whitney's U  
1079 test.

1080 **(F)** The proliferation of Treg cells of indicated genotypes, assayed by BrdU incorporation  
1081 assay (n=3 mice of three experiments; means  $\pm$  s.d., \* $p$ <0.05, \*\* $p$ <0.01, \*\*\*\* $p$ <0.0001,  
1082 by two-way ANOVA post Sidak's multiple comparisons test).

1083 **(G)** Apoptosis of WT and Dcaf1-deficient Treg cells in spleen was analyzed by flow-  
1084 cytometry using Annexin V and 7AAD staining. Left, representative sample; right,  
1085 composite data of 4 mice; n=4 mice; means  $\pm$  s.d., \*\* $p$ <0.01, \*\*\*\* $p$ <0.0001, by two-way  
1086 ANOVA post Sidak's multiple comparisons test.

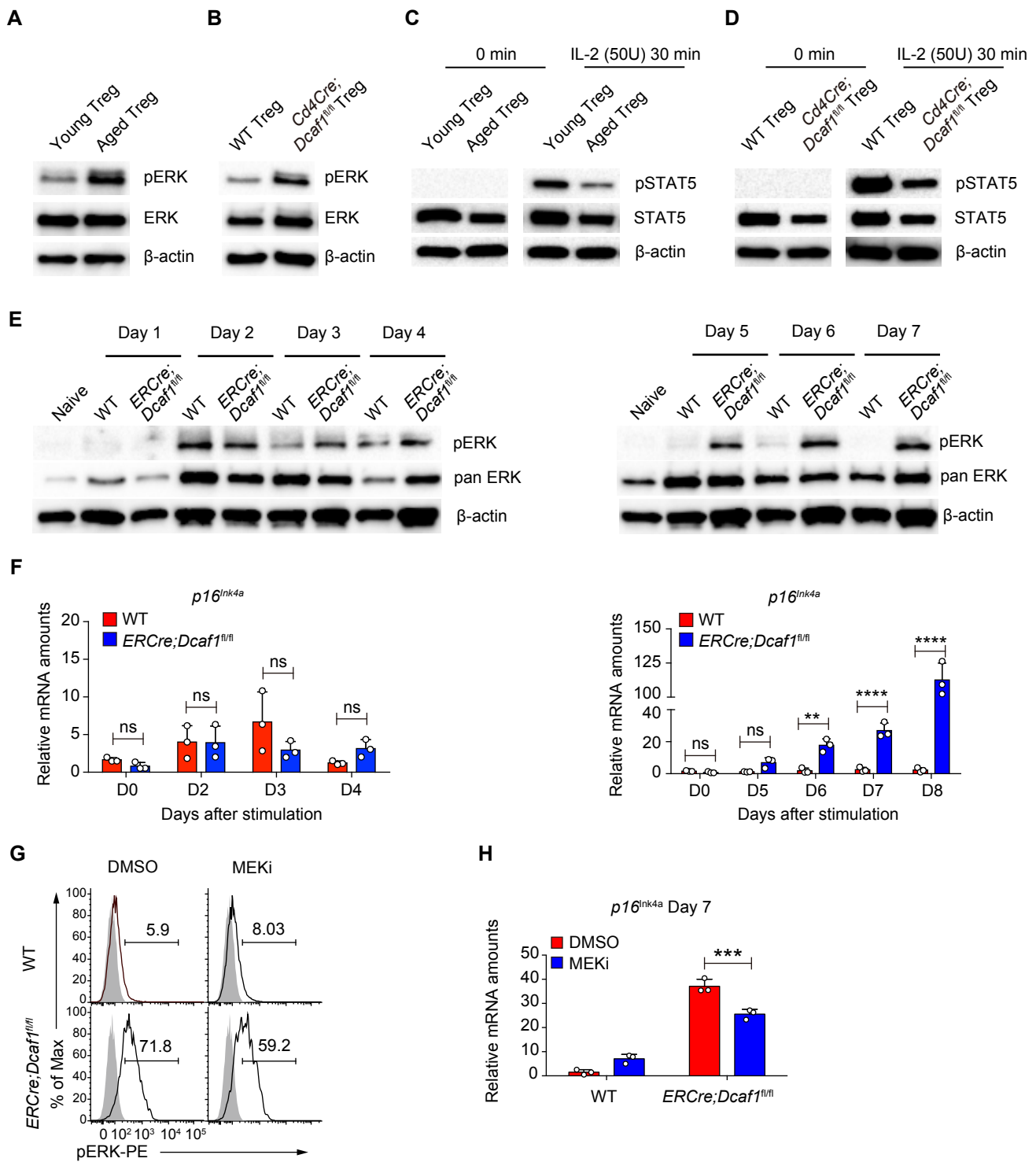
1087

Fig. S3



1088 **Fig. S4. ERK activation in aged and Dcaf1-deficient Treg cells**  
1089 **(A-B)** Immunoblotting to detect ERK phosphorylation (pERK) in Treg cells from young  
1090 and aged mice **(A)** and from wild-type and *Cd4Cre;Dcaf1<sup>fl/fl</sup>* mice **(B)**. The results are  
1091 representative of three experiments.  
1092 **(C-D)** Immunoblotting to detect STAT5 phosphorylation (pSTAT5) in Treg cells from  
1093 young and aged mice **(C)** and from wild-type and *Cd4Cre;Dcaf1<sup>fl/fl</sup>* mice with (30 min)  
1094 or without (0 min) IL-2 treatment **(D)**. Results are representative of three experiments.  
1095 **(E)** Immunoblotting to detect ERK phosphorylation (pERK) in activated wild-type and  
1096 *ERCre;Dcaf1<sup>fl/fl</sup>* CD4 T cells treated with 4-hydroxy-tamoxifen for indicated days.  
1097 Results are representative of three experiments.  
1098 **(F)** qRT-PCR analysis to determine mRNA expression of *p16<sup>Ink4a</sup>* in activated wild-type  
1099 and *ERCre;Dcaf1<sup>fl/fl</sup>* CD4 T cells treated with 4-hydroxy-tamoxifen for indicated days.  
1100 The floxed *Dcaf1* gene was removed by tamoxifen-inducible-Cre (*ERCre*) mediated  
1101 deletion in the presence of 4-hydroxy-tamoxifen (n=3 mice from three experiments;  
1102 means  $\pm$  s.d., ns, not significant, \*\* $p < 0.01$ , \*\*\*\* $p < 0.0001$ , by two-way ANOVA post  
1103 Sidak's multiple comparisons test).  
1104 **(G)** Immunoblotting to detect ERK phosphorylation (pERK) in activated wild-type and  
1105 *ERCre;Dcaf1<sup>fl/fl</sup>* CD4 T cells treated with DMSO or MEK inhibitor (MEKi) in the  
1106 presence of 4-hydroxy-tamoxifen. Results are representative of three experiments.  
1107 **(H)** qRT-PCR analysis to determine mRNA expression of *p16<sup>Ink4a</sup>* in activated wild-type  
1108 and *ERCre;Dcaf1<sup>fl/fl</sup>* CD4 T cells treated with DMSO or MEK inhibitor (MEKi) in the  
1109 presence of 4-hydroxy-tamoxifen. (n=3 mice from three experiments; means  $\pm$  s.d.,  
1110 \*\*\* $p < 0.01$ , by two-way ANOVA post Sidak's multiple comparisons test).

Fig. S4





1111 **Fig. S5. DCAF1 related pathways revealed by IP-MS**

1112 **(A)** Venn diagram to show 57 DCAF1 interacting proteins shared by T and non-T cells  
1113 identified based on two independent IP-MS studies.

1114 **(B)** Ingenuity Pathway Analysis (IPA) of top 25 canonical pathways regulated by the 57  
1115 DCAF1 binding proteins identified in **(A)**.

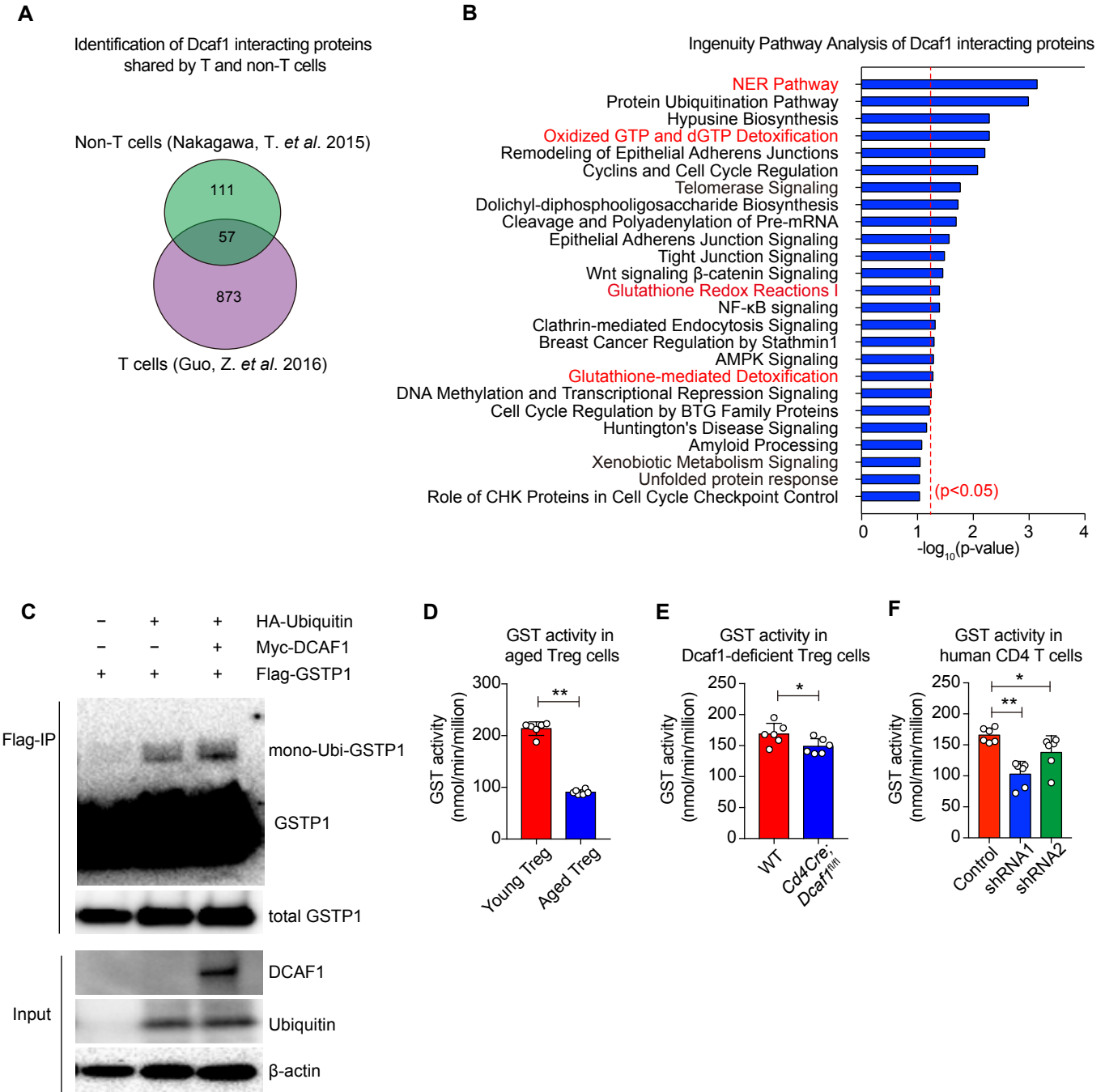
1116 **(C)** The ubiquitylation of GSTP1 in 293T cells transfected with plasmids of Myc-  
1117 DCAF1, FLAG-GSTP1 and HA-ubiquitin. The cell lysate was subjected to IP with an  
1118 antibody to FLAG under denaturing conditions (0.1% SDS). The resulting precipitates  
1119 were blotted with the anti-Myc antibody for DCAF1, anti-HA antibody for Ubiquitin,  
1120 anti-FLAG antibody for GSTP1 and nemo-ubiquitylated GSTP1.

1121 **(D)** The glutathione S-transferases (GST) activity in young and aged Treg cells; n=6  
1122 mice; means  $\pm$  s.d.,  $**p < 0.01$ , by Mann-Whitney's U test.

1123 **(E)** The glutathione S-transferases (GST) activity in WT and *Dcaf1*-deficient Treg cells;  
1124 n=6 mice; means  $\pm$  s.d.,  $*p < 0.05$ , by Mann-Whitney's U test.

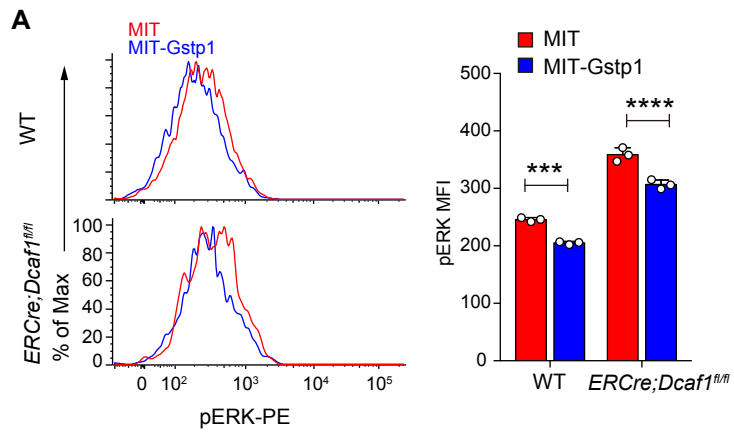
1125 **(F)** The glutathione S-transferases (GST) activity in human T cells transduced with  
1126 lentivirus expressing two shRNA targeting *Dcaf1* and scrambled control for 4 days; n=6;  
1127 means  $\pm$  s.d.,  $*p < 0.05$ ,  $**p < 0.01$ , by Mann-Whitney's U test.

Fig. S5



1128 **Fig. S6. GSTP1 suppressed ERK phosphorylation in Dcaf1-deficient T cells**  
1129 **(A)** Flow-cytometry of ERK phosphorylation (pERK) in activated wild-type and  
1130 *ERCre;Dcaf1<sup>fl/fl</sup>* CD4 T cells transduced with MIT or MIT-Gstp1 virus in the presence of  
1131 4-hydroxy-tamoxifen, analyzed by DCFDA (n=3 mice of three experiments;  
1132 representative results are shown; means  $\pm$  s.d., \*\*\* $p$ <0.001, \*\*\*\* $p$ <0.0001, by two-way  
1133 ANOVA post Sidak's multiple comparisons test).

Fig. S6



1134 **Fig. S7. Schema for the regulation of Treg cell ageing via DCAF1-GSTP1-ROS and**  
1135 **its role in immunological ageing.**

Fig. S7

